

**Silver Nanoparticle deposited screen printed electrodes coated with Schiff base ionophores as voltammetric sensors for Fe (II) and Fe (III)**

A  
Thesis submitted in  
Fulfillment of the requirement of the degree of

**Masters of Science in Chemistry**

Submitted by  
**Subhay**  
**(301702035)**

Under the Supervision  
Of

**Dr. Susheel Mittal CChem FRSC**  
**Senior Professor**



**School of Chemistry and Biochemistry**  
**THAPAR INSTITUTE OF ENGINEERING AND TECHNOLOGY**  
**PATIALA – 147004**  
**July, 2019**

---

## Certificate

---

Certified that the thesis entitled “Silver nanoparticle deposited screen printed electrodes coated with schiff base ionophores as voltammetric sensors for Fe (II) and Fe (III)” which is submitted by Ms. Subhay in partial fulfillment of the requirement for the award of the Degree of Masters of Science in Chemistry in the School of Chemistry and Biochemistry, Thapar Institute Of Engineering and Technology, Patiala, is a record of candidate's own independent and original research work carried out by her under my supervision and guidance. The material embodied in this thesis has not been submitted in part or full to any other University or Institute for the award of any other degree.

*Susheel Mittal*  
(Supervisor) 13-7-19

Dr. Susheel Mittal CChem FRSC

Senior Professor

School of Chemistry and Biochemistry

THAPAR INSTITUTE OF ENGINEERING AND TECHNOLOGY, PATIALA

(Prof. & Head)

Dr. Amjad Ali

Professor

School of Chemistry and Biochemistry

THAPAR INSTITUTE OF ENGINEERING AND TECHNOLOGY, PATIALA



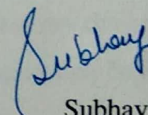


## Candidate's Declaration

---

I, hereby declare that the work presented in the thesis entitled "**Silver nanoparticle deposited screen printed electrodes coated with schiff base ionophores as voltammetric sensors for Fe (II) and Fe (III)**" in fulfillment of the requirement for the award of the Degree of Masters of Science in Chemistry, School of Chemistry and Biochemistry, Thapar institute of engineering and technology, Patiala is an authentic record of my own work carried out under the supervision of Dr. Susheel Mittal, Cchem FRSC Senior Professor, School of Chemistry & Biochemistry, THAPAR INSTITUTE OF ENGINEERING AND TECHNOLOGY, Patiala, India. The matter embodied in this thesis has not been submitted in part or full to any other university or institute for the award of any degree in India or Abroad.

Place: Patiala  
Date: July 15, 2019



Subhay  
301702035



# Acknowledgement

---

A piece of work to become perfect, one needs the blessings and help of many. For the completion of this research work, I am indebted to many for their generous contributions, be it in the form of a piece of advice or suggestions for improvement.

First of all, let me bow my head in reverent gratitude to God almighty for the manifold blessings showered on me and for the undeserving grace shown to me for the successful completion of this work.

Let me place on record my profound gratitude to my supervising guide Prof. Susheel Mittal Cchem FRSC for admitting me in to the programme. His scholarly assistance, inspiring guidance and amiable demeanor really helped me to complete the work in the stipulated time. Apart from the subject of my research, I learnt a lot from him, which I am sure, will be useful in different stages of my life. His simplicity, moral ethics, behavior towards colleagues and students inspired me a lot. Sir, I consider it as a blessing to work under you.

I would like to thank Prof. Amjad Ali, Head of the Department and I am grateful to all teachers of the department for their help and valuable suggestions. I express my sincere thanks to all the non-teaching staff of the department for the help and support they have rendered to me.

I would also like to place on record my gratefulness to all those people who have been with me since the early days of my six month research project tenure.

Ms. Sonia Rana was the chief person who kept me going at the beginning till end. Without her wholehearted support it would not have been possible me to complete this work. Let me also express my love and thanks to my dear lab mates Mrs. Madhvi Rana, Mr. Sanjeev Kumar for their support and tea breaks.

I would like to extend my gratefulness to all my friends in Chemistry and Biochemistry labs. A special thanks to Mehak, Rohini, Simran, Sagrika, Jaya Bharti for their help and support.

My thanks to the friend from other department for the help and support rendered. I thank Ms. Ravinder Kaur Sandhu for her wonderful friendship, love and care.

Literally I lack words to express my love and indebtedness to my Papa and Mumma. With their immense love, ardent prayers and constant support they have lighted my paths ever since the beginning of my life. Let me also make a special mention of Riya, my wonderful sister, who has been there for me through the thick and thin of my life. The unconditional love and encouragement provided by my beloved elder sister Mrs. Samriti Thakur Dadwal served as a secure anchor during the hard and easy times. Thank you.

*Subhay*  
**Subhay**



# List of contents

<b>S.No.</b>	<b>Contents</b>	<b>Page No.</b>
	Abstract	Vi
<b>Chapter 1</b>	<b>Introduction</b>	<b>1-4</b>
<b>Chapter 2</b>	<b>Literature Review</b>	<b>5-14</b>
2.1	Spectroscopic chemosensors	5-6
2.1.1	Schiff base as optical sensors	6-7
2.1.2	Nanoparticle based optical sensors	7
2.2	Electrochemical chemosensors	8-12
2.2.1	Nanoparticle based chemosensors	8-10
2.2.2	Ionophores as electrochemical sensor	10-11
2.2.3	Schiff base electrochemical sensor	11-12
2.3	Screen printed electrode	12-14
<b>Chapter 3</b>	<b>Materials and methods</b>	<b>15-17</b>
3.1	Chemicals used	15
3.2	Instrumentation	15
3.3	Preparation of screen printed electrode	16
3.4	Preparation of solution	16
3.5	Modification of screen printed electrode	16
3.6	Experimentation	16-17
3.7	Real life sampling	17
<b>Chapter 4</b>	<b>Results and discussion</b>	<b>18-43</b>
4.1	Optimization of experimental parameters	18
4.1.1	Optimization of silver nitrate concentration	18
4.1.2	Optimization of time of chronoamperometry	18-19
4.1.3	Optimization of potential	19
4.1.4	SEM analysis of modified SPE	21
4.2	Ion-recognition of JS-2/AgNPs modified SPE	23
4.2.1	Selection of supporting electrolyte	23
4.2.2	Electrochemical response of JS-2/AgNPs modified SPE	23-24

<b>4.2.3</b>	<b>Impact of scan rate</b>	<b>26</b>
<b>4.2.4</b>	<b>Influence of presence of different ions</b>	<b>26-28</b>
<b>4.2.5</b>	<b>Quantitative measurement of Fe (III) using SPE</b>	<b>30</b>
<b>4.2.6</b>	<b>Interference study</b>	<b>31-32</b>
<b>4.2.7</b>	<b>Real life sample study</b>	<b>33</b>
<b>4.2.8</b>	<b>Conclusions</b>	<b>34</b>
<b>4.3</b>	<b>Ion-recognition of JS-3/AgNPs</b>	<b>34</b>
<b>4.3.1</b>	<b>Supporting electrolyte selection</b>	<b>34</b>
<b>4.3.2</b>	<b>Study of surface of bare and unmodified SPE</b>	<b>34-35</b>
<b>4.3.3</b>	<b>Effect of scan rate on cathodic peak current</b>	<b>37-38</b>
<b>4.3.4</b>	<b>Sensing activity at the modified electrode</b>	<b>39</b>
<b>4.3.5</b>	<b>Detection limit of proposed sensor for Fe (III)</b>	<b>40</b>
<b>4.3.6</b>	<b>Interference study</b>	<b>41-42</b>
<b>4.3.7</b>	<b>Real life sampling</b>	<b>42-43</b>
<b>4.3.8</b>	<b>Conclusions</b>	<b>43</b>
	<b>References</b>	<b>44-53</b>

**DEDICATED TO MY PARENTS**



## ABSTRACT

In this study, voltammetric sensors for the detection of ferrous and ferric ions developed have been presented. Silver nanoparticles (AgNPs) were electrochemically deposited on screen printed electrode. Further, schiff base was drop-coated on AgNPs modified SPE. Some parameters like concentration of silver nitrate, deposition potential, deposition time were optimized before carry out further studies. Modification of the probe was characterized using scanning electron microscopy (SEM), Energy-dispersive X-ray spectroscopy (EDX), and cyclic voltammetry (CV) methods. Change in the redox behavior before and after complexation provided indication about the sensing and analyzed using CV and differential pulse voltammetry (DPV). AgNPs provided better surface for the deposition of organic moiety. JS-2 modified AgNPs-SPE was used for the sensing of ferrous ions, whereas JS-3 modified AgNPs-SPE detected ferric ions in aqueous medium. JS-2/AgNPs modified SPE detect Fe (II) in the detection range 0.0  $\mu\text{M}$  to 70.3  $\mu\text{M}$  with detection limit 0.19  $\mu\text{M}$  and JS-3/AgNPs modified SPE detect Fe (III) ions in working range of 0.0  $\mu\text{M}$  to 42.8  $\mu\text{M}$  with limit of detection 1.73  $\mu\text{M}$ . The proposed sensors worked well even in the presence of interfering ions. Practical applicability of the sensors was explored by using them for the detection of target ions in real-life samples.

## **Chapter: 1**

### **INTRODUCTION**

Sometimes, heavy metal ions which are frequently used in industries and household use are thrown as such in the environment. The chief extortions to human health from heavy metal ions are related with the exposure to cadmium, lead, arsenic and mercury. Once settled, they are stubborn in the atmosphere and their discard from sources like waste water, ambient environment is necessary to ensure clean water to drink and environment to breathe, live. Indeed, there is a need of sensors which can precisely and selectively detect these heavy metal ions.

#### **1.1 Chemical sensing**

Definition by IUPAC “A chemical sensor is a device which transforms chemical information, ranging from the concentration of a special sample component to total composition analysis, into an analytically useful signal.”As above mentioned, the chemical evidence originated from a physical property or from a chemical reaction of the analyte of the scheme which is under examination.

Chemical sensors consist of two basic functional units:

1. Transducer part
2. Receptor part

Transducer Part: It measures the electrical signal generated by the chemical process at the electrode surface. As such, transducer does not show any selectivity.<sup>1</sup>

Receptor Part: It converts the chemical evidence in to the form of energy which may be restrained by the transducer.

#### **1.2 Types of Chemical sensors**

**1.2.1.** Chemical sensors are divided into following categories, based upon the type of transducers:

**1.2.2. Optical Sensors:** These are optical devices that change the optical sensations into a useful analytical signal. These signals are the results of interaction of receptor part with an analyte.<sup>1</sup> Other name of these sensors is optodes.

**1.2.3. Electrochemical Sensor:** These are electrochemical devices which transform the electrochemical interaction between analyte and electroactive receptor at the electrode into a useful signal. Electrochemical sensors are further subdivided into following types:

- (a) Voltammetric sensors
- (b) Potentiometric sensors
- (c) Conductometric sensors
- (d) Amperometric sensors

**1.2.4. Mass Sensitive Sensors:** This type of sensors is based on the change in the mass of a substance at a particularly modified surface. Mass sensitive sensors are of two types:

- (a) Surface acoustic wave sensors
- (b) Piezoelectric devices

**1.2.5. Heat Sensitive Sensors:** Commonly, these are also well-known as calorimeter i.e. calorimetric sensors. Within a chemical reaction, heat change is monitored with transducer like platinum thermometer.

Among these sensors, electrochemical sensors and optical sensors are considered to be the powerful and more sensitive techniques.

In the proposed work, electrochemical method has been chosen in place of optical method because it has better influential, measurable electric signals as voltage or current.

Also, due to its high sensitivity, small size of equipment, onsite detection, easy installation electrochemical devices are more acceptable. Electrochemical sensors are further subdivided in different types. Among these, voltammetric sensors are used in the present study.<sup>2</sup>

Voltammetry is the best technique among all in electrochemical analysis. In this technique, potential (E) is realistic on the working polarized electrode against the reference electrode and the resulting current (A) is measured.

Voltammetry, further divided into following techniques is based on the function of potential applied on the working electrode.

Cyclic Voltammetry is one of the maximum used voltammetric methods like Staircase voltammetry, Anodic stripping voltammetry, Square wave voltammetry, Linear sweep voltammetry Cathodic stripping voltammetry, Fast scan voltammetry Normal pulse voltammetry and Differential pulse voltammetry. For obtaining extensive information regarding the electrochemical processes, electron transfer reaction mechanism can be studied by CV. In CV, during its cathodic cycle, species undergo reduction and in anodic cycle it undergoes oxidation reaction. Also, it tells us about that a reaction is reversible or not.<sup>3</sup> For a reversible reaction, peak current is given by Randles-Sevcik equation:

$$i_p = (2.69 \times 10^5) n^{3/2} A D^{1/2} C v^{1/2}$$

where, D the diffusion coefficient ( $\text{cm}^2 \text{s}^{-1}$ ),  $i_p$  is peak current at redox potential, C is the concentration of the electro active species ( $\text{mol cm}^{-3}$ ) and v is scan rate ( $\text{V s}^{-1}$ ), A is the electrode surface area ( $\text{cm}^2$ ), n is the number of electrons transferred during redox event occurring at electrode surface.

The applied potential, in differential pulse voltammetry is in a series of pulses. A fixed number of pulses of small amplitude (10 mV to 100 mV) are superimposed on a linearly increasing base potential which change slowly. Current is examined before and after the application of the pulse and plotted against base potential for each pulse.<sup>4</sup>

Working of voltammetric sensors is based on three electrode system namely reference electrode, working electrode and counter electrode. Present studies are done using differential pulse voltammetry and cyclic voltammetry.<sup>5</sup>

**1.3. Screen Printed Electrode:** In SPE, carbon ink is pasted on the polymer sheet strip made up of polycarbonate. Due to its low cost, stability, conductivity and sensitivity, this electrode is in trend and replaces the three electrodes system as these are easy to port for on-site detection.

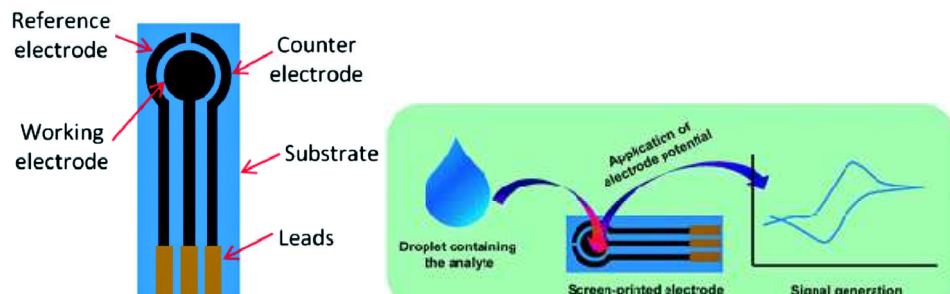


**Figure 1.1. :** Screen printed electrode (source internet)

### 1.3.1. Modification of the working electrode

In recent past years, several applications have been published on the screen printed electrodes. Modification of SPE is done in most of the cases with nanoparticles. Nanoparticles improved the working electrode surface. There are many known nanoparticles which provide good conductivity and electrocatalytic properties, which ultimately enhance the redox reaction that is taking place on the electrode surface.

Nanoparticles can be used in two ways on the electrode; either these can be synthesized using the known chemical reactions and then drop cast on the SPE, or can be directly synthesized on the SPE by some analytical means like chronoamperometry by applying the optimal potential in the presence of that specific salt and buffer.

Also, modification of the SPE is done with some electroactive ionophore such as Schiff bases or derivative of Schiff bases. These are only pasted by drop coating method on SPE and act as receptors for analytes. As a host, Schiff base makes available sufficient space for metal ions. In result, shift of waves or formation of new waves is observed. Shape and size is the main characteristic which plays role in binding of metal ion with Schiff base. If size of ion is larger than Schiff base then formation of dome like structure takes place and complete binding is not possible. On the other hand, if the size is small then also bonds are not stable because of larger size of cavity. So, the requirement proper size of host and guest is important.

## Chapter: 2

### LITERATURE SURVEY

Identification of ionic species in various sample matrixes becomes an interesting field as an important domain of supramolecular chemistry. For ion detection in biological, medicinal and environmental fields. Chemical sensors attracted lots of attention<sup>6</sup>. chemosensors can be used in association with colorimetric, fluorometric and electrochemical techniques. Chemical sensors can be designed keeping host-guest interaction in mind<sup>7</sup>. A number of moieties such as crown ether based<sup>8</sup>, cryptands<sup>9</sup>, podands<sup>10</sup>, spherands<sup>11</sup>, schiff bases<sup>12</sup> and nanoparticles<sup>13</sup> are available in literature which has been used for ion sensing. In the following section, detailed review of the literature on the basis of type of ionophore has been discussed. Our main focus will be on the schiff base ionophores because they are easy to synthesize and possess strong coordinative ability. All imine based compounds have their coordinating site through heteroatom present in its moiety which causes metal-ligand interaction and is used for metal detection. By changing the nature and position of substituent around the imine moiety, it is possible to control the size of the cavity formed for metal complexation.

The literature was classified with respect to the techniques used in chemosensors:

- (a) Spectroscopic techniques based
- (b) Electrochemical techniques based

#### 2.1. Spectroscopic chemosensors

Gupta *et al.* (2015)<sup>14</sup> proposed a coumarin based fluorescent chemosensor which was selective for Mg (II) ion even in the presence of other s-block elements. The detection limit was 0.43 $\mu$ M. Cayuela *et al.* (2016)<sup>15</sup> discovered a sensor for silver ions based upon luminescent Carbon Quantum Dot hydrogels. The detection limit (0.55 $\mu$ g mL<sup>-1</sup>) and limit of quantification (1.83  $\mu$ g mL<sup>-1</sup>) were reported. In another publication, Niu *et al.* (2016)<sup>16</sup> established a fluorescent sensor modified with carbon quantum dots/gold nanoclusters (CODs/AuNCs) which were used for detection of Cd (II) ions and L-ascorbic acid (AA). In that work, the detection limit reported for Cd (II) ions and for AA were 32.5 nM and 0.15 respectively. Xie *et al.* (2018)<sup>17</sup> synthesized nanoclusters of carbon

dots-gold for fluorescent and colorimetric determination of Hg (II) ions. In presence of Hg (II) fluorescence emission takes place that falls in the range of 2–15 nM, also the detection limit found to be 0.73 nM. Yue *et al.* (2017)<sup>18</sup> proposed a naphthalene-derived fluorescent sensor which proved to be a good for selectivity of Al (III). That specific proposed sensor shows fluorescence at 475 nm due to the presence of Al (III) having lowest detection limit 0.43  $\mu$ M owing to photo induced electron transfer.

### 2.1.1. Schiff's base as optical sensors

Kim *et al.* (2014)<sup>19</sup> published a fluorescent sensor using schiff base for selective detection of Zn (II) and Al (III), in aqueous medium. Furthermore, the detection limits claimed for the Al (III) (0.09  $\mu$ M) and for Zn (II) (6.6  $\mu$ M) are far below the guideline of the WHO. Qin *et al.* (2015)<sup>20</sup> also explored schiff base fluorescent sensor which recognizes Al(III) with LOD of  $10^{-7}$  M and Zn(II) ions. Li *et al.* (2015)<sup>21</sup> published a report on colorimetric sensor and fluorescent based on Schiff base derivative for the Al (III) ions detection. The role of hydroxyl group (OH) and amide linkage (NH) present in the ionophore for Al (III) ions binding has been explored. Yuan *et al.* (2016)<sup>22</sup> presented a triazole Schiff base derivative as fluorescent sensor showed a good selectivity for Zn (II). He obtained the limit of detection of 51 nM with the help of UV-Vis titration. Tang *et al.* (2017)<sup>23</sup> developed fluorescent sensor with schiff base moiety for Zn (II), Fe (III), Cu (II) detection in different solvents. Cu(II) shows the limit of detection  $8.27 \times 10^{-8}$  M in EtOH/H<sub>2</sub>O, while Fe(III) and Zn(II) gives detection limit  $2.12 \times 10^{-7}$  M and  $6.64 \times 10^{-7}$  M, respectively in ethanol system. Liu *et al.* (2018)<sup>24</sup> also published a report on fluorescent sensor based on schiff base obtained by the reaction of picolinohydrazide and 4-(diethylamino)salicylaldehyde. That specific sensor showed selectivity with Al (III) and Zn (II). The limit of detection reported by this group was and for Al (III) ( $8.30 \times 10^{-8}$  M) and Zn (II) ( $1.24 \times 10^{-7}$  M) respectively. Wang *et al.* (2018)<sup>25</sup> developed quinoline-base Schiff base fluorescent sensor for detection of Al (III) with detection limit  $8.08 \times 10^{-8}$  M analyzed in methanol. Zhu *et al.* (2019)<sup>26</sup> synthesized a schiff base sensor for Fe (II), Fe (III) and Cu (II) ions. The detection limits for Fe (III) ( $2.17 \times 10^{-6}$  M), and for Fe (II) ( $2.06 \times 10^{-6}$  M) and for Cu (II) ( $2.48 \times 10^{-6}$  M), respectively. Zhang *et al.* (2019)<sup>27</sup> recently presented colorimetric schiff base sensor which reported detection of Al (III), Fe (III), Cu (II) and Cr (III) ions. The detection limits for ions Cu (II), Cr (III), Fe

(III) and Al (III) were,  $4.65 \times 10^{-7}$  M,  $3.37 \times 10^{-7}$  M,  $3.58 \times 10^{-7}$  M and  $4.89 \times 10^{-7}$  M, respectively.

### 2.1.2. Nanoparticle based optical sensors

Mahajan *et al.* (2015)<sup>28</sup> used *N*-methyl isatin nanoparticles for the development of fluorescent probe selective for Cd (II) (DL 1.33  $\mu\text{g}/\text{mL}$ ) due to electrostatic interaction between nanoparticle probe and Cd (II). Shellaiah *et al.* (2016)<sup>29</sup> published work on colorimetric sensor modified with 3–5 nm sized gold nanoparticles obtained by reduction methods. Proposed sensor used for detection of Cr (III) with limit of detection was 13.42 nM. Shen *et al.* (2017)<sup>30</sup> discovered silver nanoprisms based Tb (III) fluorescent sensor which was highly selective for dopamine. Recorded fluorescence emission in the range of 0.6–100 nM and detection limit was 0.22 nM. Salami *et al.* (2018)<sup>31</sup> proposed a colorimetric sensor using modification with gold nanoparticle reported for selective determination of Fe (II) and Cr (III) ions in aqueous solutions. In aqueous solution detection limit found to be for Cr (III) and Fe (II) was 23.66 and 11.21 nM respectively. Wang *et al.* (2018)<sup>32</sup> presented a fluorescent and colorimetric based sensor modified with gold nanoparticle for the recognition of Cu (II) ions and detection limit found as 77 nM, at pH 4.

Pinyorosphatum *et al.* (2019)<sup>33</sup> proposed a paper base colorimetric sensor for phosphate ions detection. Sensor was based on anti-aggregation of 2-mercaptoethanesulfonate-modified silver nanoparticles (MS-AgNPs) in the presence of phosphate ions. Sensing mechanism was done by doing analysis of aggregation and anti-aggregation using FT-IR, TEM and UV-VIS spectroscopy. This detection limit was found as 0.33  $\text{mg L}^{-1}$  with limit of quantification 1.01  $\text{mg L}^{-1}$  and method was applied to detect phosphate in soil samples. Similarly, Wu *et al.* (2019)<sup>34</sup> reported sensor gold nanoparticles modified with 4-mercaptophenylboronic were synthesized using one-pot reaction. This colorimetric sensor illustrated selectivity towards fluoride ions. Workable range of the sensor was found in range 10.0 – 30.0  $\mu\text{M}$  with limit of detection  $3.45 \times 10^{-7}$  M. Furthermore, analytical application of the sensor was performed by analyzing the fluoride anion present in tap water, ground water and samples of human serum.

## 2.2. Electrochemical chemosensor

Electrochemically sensing probes can be used in wide range of areas. Chemically modified voltammetric electrodes have found numerous applications and therefore number of reports are available in literature regarding the detection of different analytes found in different matrices including environmental samples, food additives, pharmaceutical, clinical samples. Modification enhanced sensitivity of the electrode surface and therefore exhibits various applications.

### 2.2.1. Nanoparticle based chemosensors

Recent reports for heavy metal ions detection were published by Ruecha *et al.* (2015)<sup>35</sup>. They proposed grapheme polyaniline nanocomposite electrode as for the detection of selective sensors Zn (II), Pb (II) and Cd (II) ions. Detection limit was marked by this group for Zn (II), Cd (II) and Pb (II) 1, 0.1 and 0.1  $\mu\text{g L}^{-1}$  respectively

Lin *et al.* (2015)<sup>36</sup> explored nanoporous gold nanoparticles modified indium tin oxide glass as sensor. Differential pulse anodic stripping voltammetric sensor for Hg (II) detection in HCl solution was developed. Using optimized experimental parameters, calculated detection limit was 0.03  $\mu\text{g/L}$ . Also, the proposed sensor did not experience any interference and found analytical application. Lee *et al.* (2016)<sup>37</sup> developed electrochemical sensor for Cd (II), Pb (II), and Zn (II) ions using iron oxide and grapheme nanocomposite.  $\text{Fe}_2\text{O}_3$  and graphene nanocomposites were prepared by solvent less method. Under optimal conditions, detection limit was marked at for Cd (II), Zn (II) and Pb (II) ions 0.08  $\mu\text{g L}^{-1}$ , 0.11  $\mu\text{g L}^{-1}$  and 0.07  $\mu\text{g L}^{-1}$ , respectively.

Veerakumar *et al.* (2016)<sup>37</sup> fabricated modified glassy carbon electrodes (GCEs) with Pd nanoparticle incorporated porous activated carbons (PACs). This sensor was used for the detection of Pb (II), Cd (II), Hg (II) and Cu (II) ions with detection limit values of 41 nM, 50 nM, 66 nM and 54 nM, respectively. Real life sample analysis was done using milk samples. Romih *et al.* (2017)<sup>38</sup> reported an electrochemical electrode fabricated using a film of bismuth oh working electrode. That proposed sensor was selective towards Zn (II) with ultralow detection limit 0.15  $\mu\text{g L}^{-1}$ . P.shetti *et al.* (2017)<sup>39</sup> testified detection of clozapine using an electrochemical sensor modified with 0.8% ruthenium

doped titanium oxide nanoparticle. The designed sensor depicts high sensitivity with limit of detection 0.43 nM. The application of sensor was tested in tablets and spiked urine samples. Yuan *et al.*(2017)<sup>40</sup> developed glassy carbon electrode based electrochemical biosensor modified with chitosan, gold nanoparticle and aptamer, which exhibited good sensitivity, selectivity towards Cd (II) ions over a linear range (0.001 nM to 100 nM) along with detection limit 0.04995 pM estimated using differential pulse voltammetric data. Satisfactory results were obtained from the biosensor when tested Cd(II) ions present in tap water. Simpson *et al.* (2018)<sup>41</sup> synthesized carbon nanoparticle modified glassy carbon as electrochemical sensor, which was used to detect heavy metal ions using voltammetry method of square wave anodic stripping . The modified sensor was magnificently used for detection of Cd (II) and Pb (II) in sample of spiked water with recovery percentage 98.2% and 96.7%, respectively. Further, Marie *et al.* (2018)<sup>42</sup> fabricated a sensor based on zinc oxide nanoparticles which were functionalized with ferric oxide and used for detection of Glucose. Solution of phosphate buffer at room temperature linear range for Glucose was 100–400 mg dL<sup>-1</sup>, the limit of detection was marked 0.95 mmol L<sup>-1</sup>. Cao *et al.* (2018)<sup>43</sup> detected antigen C-reactive protein using zinc oxide nanoparticles. They measured the lowest detection limit of antigen as 1 ng/ml. Whereas, Zhu *et al.*(2018)<sup>44</sup> modified a glassy carbon electrode for simultaneous determination of 2,4,6-trichlorophenol and 4-chlorophenol. The detection limit for 2, 4, 6-trichlorophenol and 4-chlorophenol 1.55 μM and 3.69 μM, respectively. Modified sensor used for untreated tap water analysis.

Chen *et al.* (2019)<sup>45</sup> published BiSn alloy nanoparticles modified electrode as analytical sensor for selective detection of Cd (II). High sensitivity of modified probe was probably because of high conductivity, large surface area, robust cation exchange ability and abundance of active sites. Detection limit for cadmium ions was 3 nmol L<sup>-1</sup>. Zainulet *al.* (2019)<sup>46</sup> by the means of electrochemical methods prepared a multiwalled carbon electrode modified with zinc and aluminiumnanocomposite layered double hydroxide-quinclorac for the selectivity of bisphenol A without any interference. This modified sensor showed lowest detection limit at  $4.4 \times 10^{-9}$  M. Likewise, Singh *et al.* (2019)<sup>47</sup> investigated a nanoimmuno sensor for the detection of 17β-Estradiol by modifying it

with rod shaped zinc-oxide nanoparticle. With excellent performance and stability and high sensitivity for limit of detection  $0.01 \text{ pg mL}^{-1}$ .

### **2.2.2. Ionophores as electrochemical sensor**

Liao *et al.* (2015)<sup>48</sup> discovered a sensor for selective detection of Hg (II) by modifying glassy carbon electrode with carbon nanofiber with  $0.3 \text{ nM}$  as detection limit. Acceptable results were obtained while detecting Hg (II) with the proposed sensor from the Yellow River. For electrochemical sensing of  $\text{H}_2\text{O}_2$ , Zhang *et al.* (2016)<sup>49</sup> proposed a sensor modified with reduced graphene oxide supported nanoclusters of tin oxide. The sensor gave linear working range  $0.5$  to  $800 \text{ }\mu\text{M}$  with limit of detection for  $\text{H}_2\text{O}_2$  as  $478 \text{ }\mu\text{M}$ . Zhou *et al.* (2016)<sup>50</sup> reported a sensor modified with l-cysteine/graphene. Reported sensor gives selective detection of heavy metal ions like Cd (II) and Pb (II) ions with  $0.45$  and  $0.12 \text{ }\mu\text{g/L}$  detection limits, respectively. Also, Sadak *et al.* (2017)<sup>51</sup> fabricated a glassy carbon electrode by hybridizing partially oxidized graphene sheets with Nile red. Proposed sensor was used for detecting Fe (III). Detection limit was found  $18.7 \text{ nM}$ , also real life sampling was done on red wine.

Shi *et al.* (2017)<sup>52</sup> proposed a sensor for detecting Bisphenol A. Reduced graphene oxide and cuprous oxide nanocomposites were used to modify the glassy carbon electrode. Detection limit for bisphenol A by the rgo- $\text{Cu}_2\text{O}$  modified sensor was found to be  $5.3 \times 10^{-8} \text{ M}$ .

In another work done by Dahaghin *et al.* (2018)<sup>53</sup>, modified an electrode with  $\text{GO@Fe}_3\text{O}_4@2\text{-CBT}$  nanocomposites, reported as sensor for Cd (II) and Pb (II) using voltammetry. This electrode can determine cadmium and lead with detection limits  $0.02 \text{ ng mL}^{-1}$  and  $0.03 \text{ ng mL}^{-1}$  in aqueous medium.

Gevaerdet *et al.* (2018)<sup>54</sup> developed a mimic of enzymatic active site for the detection of progesterone using voltammetry. Limit of detection was found to be  $68 \text{ nmol L}^{-1}$  also limit of quantification found  $210 \text{ nmol L}^{-1}$ . It was highlighted that modified electrode has high sensitivity as compared to unmodified electrode.

Dahaghin *et al.* (2018)<sup>55</sup> designed a glassy carbon electrode for the selective determination of Cd (II) ions. IIP-NP was designed using co-precipitation polymerization methodology, in acetonitrile. Further, Cd (II) ions were leaked out with HCl and provide some moieties for Cd (II) sensing. Differential pulse voltammetric sensor gives detection

limit of  $1 \times 10^{-4} \mu\text{M}$  in different spiked environmental water. Chen *et al.* (2019)<sup>56</sup> prepared  $\text{Fe}_3\text{O}_4$  core protected into a metal-organic framework shell. Reported electrode showed electrocatalytic activity towards chlorogenic acid. Under optimal conditions, limit detection was found  $0.05 \mu\text{mol L}^{-1}$ . Rawoolet *et al.* (2019)<sup>57</sup> demonstrated a physically modified electrode using copper encapsulated organic metal framework for the determination of rifampicin and isoniazid with detection limit found for rifampicin and isoniazid was  $0.28 \text{ nM}$  and  $0.37 \text{ nM}$ , respectively and sensor was cast-off to determine them in medicinal samples like urine and blood serum samples.

### 2.2.3. Schiff base electrochemical sensor

Nourifard *et al.* (2015)<sup>58</sup> discovered an electrochemical sensor based on a new bis-Schiff base ionophore which has been synthesized by reaction of the 5-bromo salicylaldehydewith 2,6-diamino pyridine at ethanol under refluxing. Developed sensor was used for detection of ions such as  $\text{Cd (II)}$ ,  $\text{Hg (II)}$  and  $\text{Cu (II)}$  in water samples.  $0.0347$ ,  $0.0524$  and  $0.0450 \text{ ng cm}^{-3}$  were the detection limits observed for  $\text{Cd (II)}$ ,  $\text{Hg (II)}$  and  $\text{Cu (II)}$  respectively. On interference study it was observed that  $\text{Pb (II)}$  ion was interfering with  $\text{Cu (II)}$  ions. Pazalja *et al.* (2016)<sup>59</sup> developed a sensor for sensing L-cysteine in pharmaceutical products. Reported sensor was synthesized with  $\text{Ru(III)}$  Schiff base complex on carbon paste screen printed electrode. This electrode showed limit of detection ( $0.11 \text{ mg L}^{-1}$ ). Gorczynski *et al.* (2016)<sup>60</sup> proposed  $\text{Mg (II)}$  Schiff base complex modified sensor for the selective detection of dopamine in the existence of some interfering species like uric acid and ascorbic acid. Reported sensor was very sensitive and has limit of detection  $6.8 \times 10^{-9} \text{ M}$ . Ourari *et al.* (2017)<sup>61</sup> modified electrode with newly synthesized copper Schiff base complex. Proposed sensor was used for sensing of  $\text{NO}_2^-$  and  $\text{BrO}_3^-$ , and could be helpfully used to detect nitrite concentration in a linear range ( $2\text{--}14 \text{ nM}$ ) ( $R^2 = 0.992$ ) with a detection limit ( $1.5 \text{ nM}$ ). Yuan *et al.* (2017)<sup>62</sup> reported schiff base for modification of electrode which was further used for sensing of  $\text{Co (II)}$  from waste water.

Rahman *et al.* (2018)<sup>63</sup> proposed a  $\text{Sb (III)}$  sensor based on electroactiveionophore Schiffbase known as 1,1'-(-naphthalene2,3diylbis(azanylylidene))bis(methanylylidene))bis(naphthalen-2-ol) prepared by condensation reaction. Proposed sensor showed good selectivity and sensitivity for  $\text{Sb (III)}$  ions even in the existence of other interfering ions.

The detection limit was observed 0.075 nM. Bharathi *et al.* (2018)<sup>64</sup> developed a sensor to detect paracetamol. An electrode was modified with Cr (III) Schiff base complex. Proposed sensor showed good electrocatalytic activity towards paracetamol. Wang *et al.* (2018)<sup>65</sup> developed a sensor based on conjugated schiff base polymer (CSBP). Proposed sensor used three-dimensional macroporous carbon (3D-KSCs/CSBP) combined electrode for glucose sensing. Sensing for glucose was explained using detection limit 1.12  $\mu\text{M}$  with sensitivity 2.95  $\text{mA cm}^{-2} \text{mM}^{-1}$ . Mohan *et al.* (2019)<sup>66</sup> explored sensor based on thiosemicarbazide schiff base for Pb(II) ion-selective electrodes. Reported sensor can be operated over a wide concentration range ( $1.0 \times 10^{-7}$  -  $1.0 \times 10^{-2}$  M). Detection limit was marked ( $4.0 \times 10^{-8}$  M), also sensor was being tested on different water samples.

Wang *et al.* (2019)<sup>67</sup> used condensation reaction to produce electroactive Schiff base polymers (SBP<sub>Thi</sub>). This probe aimed at electrochemical sensing of glucose with limit of detection 0.27  $\mu\text{M}$ . The SBP<sub>Thi</sub> being porous used for glucose loading and electrode modification. SBP<sub>Thi</sub>/GOD flexible electrode can use to determine glucose in sweat. Aqlan *et al.* (2019)<sup>68</sup> used Tetradentate Schiff base as ionophore for the detection of Pb (II) in phosphate buffer, solution. Ionophore was deposited uniformly on the glassy carbon electrode.

### 2.3. Screen printed electrode (SPE)

Lzadkhah *et al.* (2015)<sup>69</sup> published his work on schiff base fabricated SPE for the sensitivity of Cu (II) ions from the environment. The detection limit was found (0.01  $\mu\text{g L}^{-1}$ ) and quantification limit (.06  $\mu\text{g L}^{-1}$ ). Nourifard *et al.* (2015)<sup>58</sup> described the preparation of Schiff base modified screen printed electrode. Authors synthesize new bis-Schiff base ligand, with the reaction of 5-bromo salicylaldehyde with the 2, 6-diamino pyridine at ethanol while refluxing. Proposed sensor had good selectivity for Cd (II), Hg (II) and Cu (II) ions with detection limits (0.0347  $\text{ng cm}^{-3}$ , 0.0524  $\text{ng cm}^{-3}$  and 0.0450  $\text{ng cm}^{-3}$ ). Parsaei *et al.* (2015)<sup>70</sup> synthesized an electrochemical sensor for the selectivity of nitrite ion. Modification of SPE was done with magnetite nanospheres and Co(II) Schiff base complex. The limit of detection was found to be  $1.5 \times 10^{-2} \mu\text{mol L}^{-1}$ . Real life analysis was tested on water samples. Jahani *et al.* (2016)<sup>71</sup> proposed a nickel oxide nanoparticle incorporated grapheme nanosheet modified screen printed electrode

(NiO/GR/SPE), for dopamine and uric acid detection. Limit of detection for dopamine was calculated using change in anodic peak current which was found as  $3.14 \times 10^{-7}$  M with range of concentration (1.0–500.0  $\mu$ M).

Chaiyo *et al.* (2016)<sup>72</sup> developed an electrochemical sensor, graphene modified SPE which was used for the detection of heavy metal ions such as Cd (II), Zn (II) and Pb (II) ions. The detection limits of  $0.08 \text{ ng L}^{-1}$ ,  $0.06 \text{ ng L}^{-1}$  and  $0.09 \text{ ng mL}^{-1}$  for Pb (II), Cd (II) and Zn (II) ions were observed, respectively. Beitollahi *et al.* (2016)<sup>73</sup> fabricated a Graphene Oxide/ZnO Nano Composite screen printed carbon electrode. Proposed sensor shows electrocatalytic activity towards Levodopa and Tyrosine with limit of detections of  $3.4 \times 10^{-7}$  M and  $4.5 \times 10^{-7}$  M, respectively. Rana *et al.* (2017)<sup>74</sup> presented a disposable electrode for detection of Al (III) ions modified with Schiff base ionophore. Observed detection limit was  $2.26 \text{ ng L}^{-1}$ . Real life sample analysis of proposed sensor for Al (III) was checked in water samples. Mehta *et al.* (2017)<sup>75</sup> reported an electrochemical sensor created on quantum dots modified screen printed electrode. Developed sensor showed selectivity for parathion even in the presence of its metabolite, paraoxon. Ultrasensitive sensor for parathion has limit of detection at  $46 \text{ pg/L}$ . Reddy *et al.* (2018)<sup>76</sup> proposed an analytical sensor for the selective detection of uric acid by modifying carbon paste electrode in the presence of dopamine in addition to ascorbic acid. The reported electrochemical sensor has detection limit of  $0.4 \mu\text{M}$ .

Jianet *et al.* (2018)<sup>77</sup> described modified screen-printed electrodes using reduced graphene oxide and gold nanoparticles for the investigation of nitrite in food. Reported sensor was highly sensitive and limit of detection was found  $0.13 \mu\text{M}$ . Jeromiyas *et al.* (2018)<sup>78</sup> developed screen printed electrode modified with bismuth nanoparticles. Reported electrode showed its significant activity towards Hg (II) with Limit of detection obtained by proposed sensor was  $0.2 \text{ nM}$ . Also, real life sampling was done with fish oil tablet, tap water, urine samples and human serum. Which gave satisfactory results. Baccarin *et al.* (2018)<sup>79</sup> electrochemically detected dopamine in existence of uric acid on the modified surface of screen printed electrode. The detection limit for dopamine was  $5.7 \times 10^{-7}$  M. Rosal *et al.* (2019)<sup>80</sup> developed an electrochemical sensor based on modification with dimethylglyoxime by drop coating on screen printed electrode. Reported sensor successfully detected Ni (II) and detection limit was found as  $2.3 \mu\text{g L}^{-1}$ . Real life

sampling was done on waste water which is in satisfactory agreement with the proposed sensor. Parsa *et al.* (2019)<sup>81</sup> developed an electrochemical sensor by incorporation of nickel oxide nanoparticles on screen printed electrode. Proposed sensor detected tyrosine with observed limit of detection 0.1  $\mu\text{M}$ . Yao *et al.* (2019)<sup>82</sup> established a disposable electrochemical sensor with the help of carbon nanohorns on screen printed electrode. This modified electrode was functionalized to detect Pb (II) and Cd (II) ions. Limit of detection was 0.4  $\mu\text{g L}^{-1}$  and 0.2  $\mu\text{g L}^{-1}$  for Pb (II) and Cd (II) ions, respectively. In addition, sensitivity of proposed sensor was successfully tested on real life samples like honey and milk samples which gave satisfactory results.

## Chapter: 3

### MATERIALS AND METHODS

#### 3.1. Chemicals Used

All reagent and solvents used for electrochemical sensing were of analytical grade and were used without further purification. All chemicals and reagents were purchased from LOBA Chemie and Sigma-Aldrich. Nitrate (LobaChemie, India) and perchlorate salts (Sigma-Aldrich) of the metal were used for cation interaction investigations. For all experiments, ultra-pure water was used. Before using any glassware, they were all cleaned with nitric acid and washed carefully with water ( $0.055 \mu\text{S}/\text{cm}$  at  $25^\circ\text{C}$ ) followed by rinsing with double-distilled water. Our coworkers synthesized the compounds JS-2 and JS-3 used (Figure 3.1).

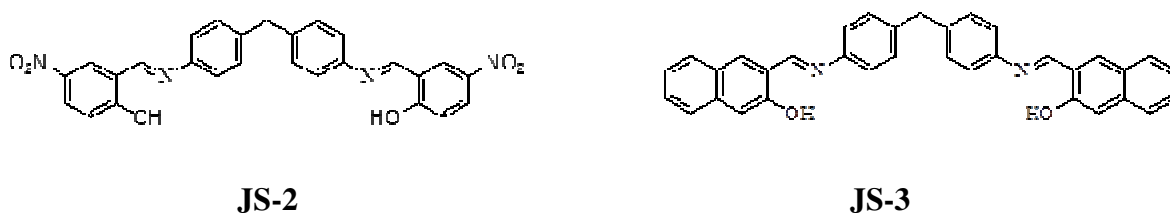


**Figure 3.1** Structures of ionophores

#### 3.2. Instrumentation

All the analytical studies were performed using miniaturized modified screen printed electrodes (SPE) by means of differential pulse voltammetry (DPV) and cyclic voltammetry (CV). For electrochemical modification, chronoamperometric technique was used. For the measurements, SPE was attached to the potentiostat (Autolab/PGSTAT12/Eco Chemie/Netherlands) via 3-electrode system connector. Experiments were carried by dropping  $40 \mu\text{L}$  of prepared solution on the electrode's active surface with the help of micropipette. All the electrochemical studies were carried out at room temperature. Emission scanning electron microscope (SEM) (JSM-6510LVfield) was used to investigate the surface morphology of modified SPE and further, energy dispersive X-ray (EDX) spectroscopy (INCA x-act Oxford) used for the investigation of elemental analysis was investigated by

### **3.3. Preparation of screen printed electrodes**

In this study, Screen Printed Electrodes (SPEs) were used to carry out all the experiments with the dimensions (41 mm×7 mm) and these SPEs were composed of three electrode system: reference electrode, counter electrode and a working electrode. These SPEs were prepared in the laboratory of Professor Craig E. Banks (Manchester Metropolitan University, UK on request). The microDEK1760RS screen-printing machine (DEK, Weymouth, UK) was used for printing. At first, a carbon-graphite ink formulation (product code: C2000802P2; Gwent Electronic Materials Ltd, UK) was printed onto a substrate of polyester (Autostat, 250 micron thickness). This layer was further dried in the fan oven at 40 °C for about half an hour. Then reference electrode Ag/AgCl was comprised by Ag/AgCl paste screen printing (product code: C2040308P2; Gwent Electronic Materials Ltd, UK) onto a substrate of plastic. Lastly, a paste of dielectric was printed onto the substrate of polyester to shield networks.

### **3.4. Preparation of solutions**

The suspensions of ionophores were made in acetonitrile having concentration  $1 \times 10^{-3}$  mol L<sup>-1</sup>. Similarly, stock solutions of the cations and anions were made having concentration  $1 \times 10^{-2}$  M. The required concentration was reached by dilution. For the preparation of stock solution double distilled water was used.

### **3.5. Modifications of screen printed electrodes**

AgNPs were analytically synthesized at the working electrode surface of SPE using chronoamperometric technique. After optimization, silver nitrate ( $10^{-4}$  M) along with Britton-Robinson buffer was added on electrode surface and accumulation potential of -1.2 V was swept for 400 s. Silver nanoparticles (AgNPs) modified SPE was further modified with respective ionophore by drop-coating 5-10 μL of suspension prepared in acetonitrile on working electrode followed by evaporation in order to dry the surface.

### **3.6. Experimentation**

All the experiments were done on the schiff base ionophore/AgNPs modified SPEs. Cyclic voltammetry (CV) and Differential pulse voltammetry (DPV) experiments were conducted using KCl (0.1 M), as supporting electrolyte. Desired solution (40 μL) was dispersed. Initially, potential range was optimized by sweeping potential between +2.0 to

-2.0 V. Further, experiments were conducted in the initial range of applied potential +1.5V to -1.5V in which distinct peaks were observed. For the recognition of metal ion sensing, preliminary studies were conducted using 10  $\mu\text{L}$  of metal ions solution with 30  $\mu\text{L}$  of an electrolyte. For the construction of calibration curve for target analyte, successive additions of required dilute solution were done at regular intervals. Cleaning of the used SPE was done using EDTA solution (0.1 M) using CV.

### **3.7. Real-life sample preparation**

In command for the estimate of practical applicability of the modified electrodes, analytes were analyzed in real-life samples. Procedures for extraction of heavy metal ions present in aqueous medium have been explained in the respective sub-section of results and discussion chapter.

## Chapter: 4

### RESULTS AND DISCUSSION

#### 4.1. Optimization of experimental parameters

Before conducting sensing experiment various parameters like amount of silver nitrate used, accumulation time and applied voltage for the modification of SPE with silver nanoparticles have been studied and appropriate parameters were optimized. Further, amount of ionophore used for drop coating was also optimized. Britton-Robinson buffer of pH 2 was used during deposition as it was reported that silver deposition at the carbon electrode surface takes place at very acid conditions.<sup>83</sup>

##### 4.1.1. Optimization of silver nitrate concentration

In order to obtain better deposition of the silver nanoparticle on the electrode surface, concentration of silver nitrate was optimized by adding different volumes of  $\text{AgNO}_3$  ( $1 \times 10^{-3}$  M) solution in Britton-Robinson (pH 2) buffer. The graph recorded using chronoamperometric technique is shown in Figure 4.1.1. With increasing amount of silver nitrate surface morphology of the working electrode in SPE changed with increase in roughness. In concern to the quality of deposition of AgNPs films, i.e., the change in roughness was monitored with change in concentration of silver nitrate. With accumulation of nanoparticle there are more active sites available for electron exchange on the surface area of electrode.<sup>84</sup> At 0.67 mM concentration maximum roughness was observed. On the basis of chronoamperometric pattern and the response of the ionophore used for modification, 0.67 mM was the optimized amount of  $\text{AgNO}_3$  used.

##### 4.1.2. Optimization of time of chronoamperometry

In order to optimize the deposition time, Ag nanoparticles were deposited by carrying out the electrodeposition for different time intervals. Chronoamperometric scans were recorded for different time periods 50 s, 100 s, 300 s, 400 s and 500 s. Figure 4.1.2, shows the electrodeposition curve for silver nanoparticles (AgNPs) synthesized using -1.2 V as bias potential for different time intervals. It was found that with increasing the deposition time, surface roughness increased and maximum roughness for AgNP was observed for 300 s. After 300 seconds, roughness of the surface decreased accompanied

with decrease of current was observed. Hence, optimized time selected for the deposition of AgNPs film in further studies was 300 s.

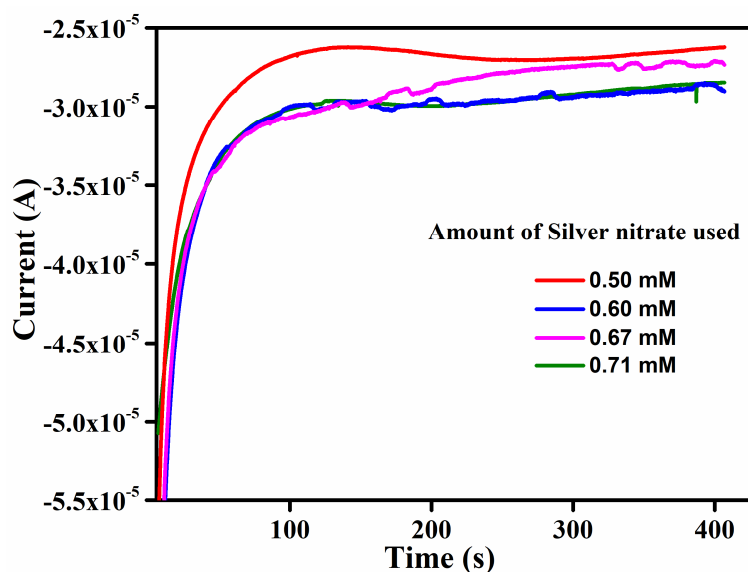


**Figure 4.1.1** Chronoamperometric plots showing response in presence of different concentrations of  $\text{AgNO}_3$  used for electrode modification. (Potential used  $-1.2$  V for 400 s)

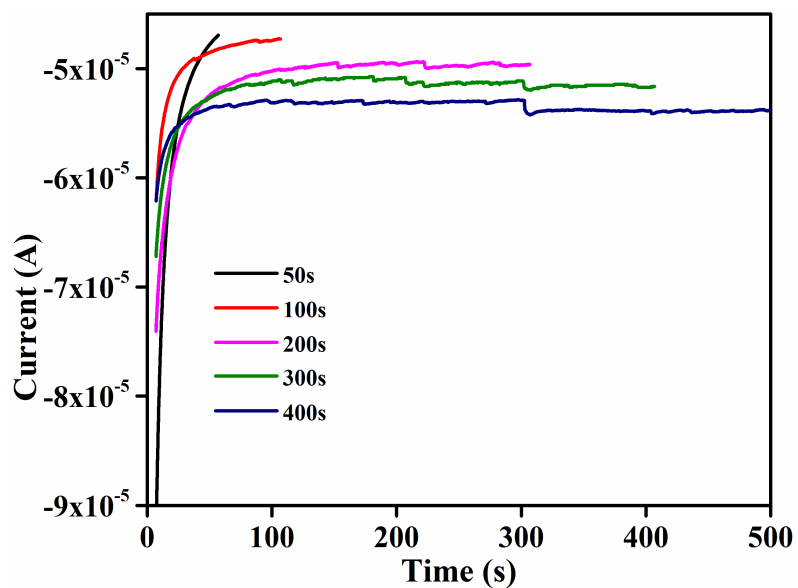


**Figure 4.1.2** Chronoamperometric plots showing electrode response at different deposition time applied for modification. (Potential used  $-1.2$  V)

### 4.1.3. Optimization of potential

In order to get, the most optimized biased potential from the deposition of AgNPs on working electrode of SPE, experiments were conducted at various applied potentials falls in range of -0.8 V to -1.4 V (biased potential). These experiments were conducted using separate SPEs for each applied potential. The output current using chronoamperometry varied between  $-1.0 \times 10^{-5}$  A to  $-1.75 \times 10^{-5}$  A. at different applied potential -0.8 V, -0.85 V and -0.9 V whereas the current varied in the range of  $-2 \times 10^{-5}$  A to  $2.75 \times 10^{-5}$  A for applied potentials of -1.0 V, -1.1 V and -1.2 V. further, for applied potential of -1.3 V and -1.4 V current  $4 \times 10^{-5}$  and  $8 \times 10^{-5}$  were recorded. It can be seen that the current varied very little in the first group of applied potentials than the second group of applied potentials. Although the output current is expected to be the same for the reduction of Ag (I) ions in to solid Ag ( as nanoparticle), yet due to different surface area of the working electrodes. A little variation is possible as separate SPE strips were used for each experiment. The greater variation in current at higher potential might be due to polarization effects likely to set in with greater applied potential. For very high-applied potentials of -1.3 V and -1.4 V. the excessively large amount of current may be due to the onset of more and more side reactions becoming feasible. From the previous studies and present experiments -1.2 V was selected for electrodeposition of AgNPs.

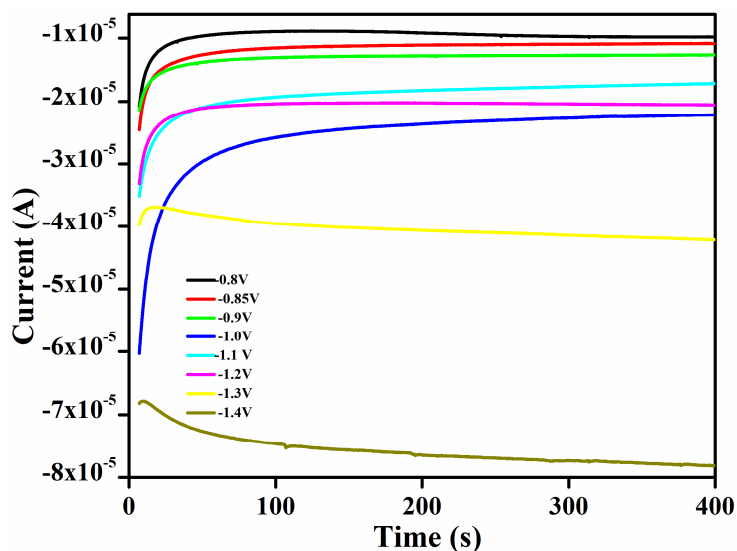


**Figure 4.1.3** Chronoamperometric plots showing response at different applied potentials used for modification at 400 s.

#### 4.1.4. SEM analysis of modified SPE

Surface morphology and the elemental analysis of working electrode before and after modification was analyzed using scanning electron microscopy (SEM) and energy-dispersive X-ray analysis (EDX). As shown in Figure 4.1.4 SEM images confirm the formation of silver nanoparticles (AgNPs) at the surface of SPE. In comparison to plain SPE, AgNPs modified SPE can be seen with white particles indicating the presence of AgNPs. EDX data also illustrated the presence of silver at the electrode surface. Electrodeposition of AgNPs also analyzed by cyclic voltammetry using 0.1 M KCl as supporting electrolyte. The AgNPs deposited SPE exhibited a clear anodic peak with potential of 0.22 V, which is the typical oxidation peak for silver.

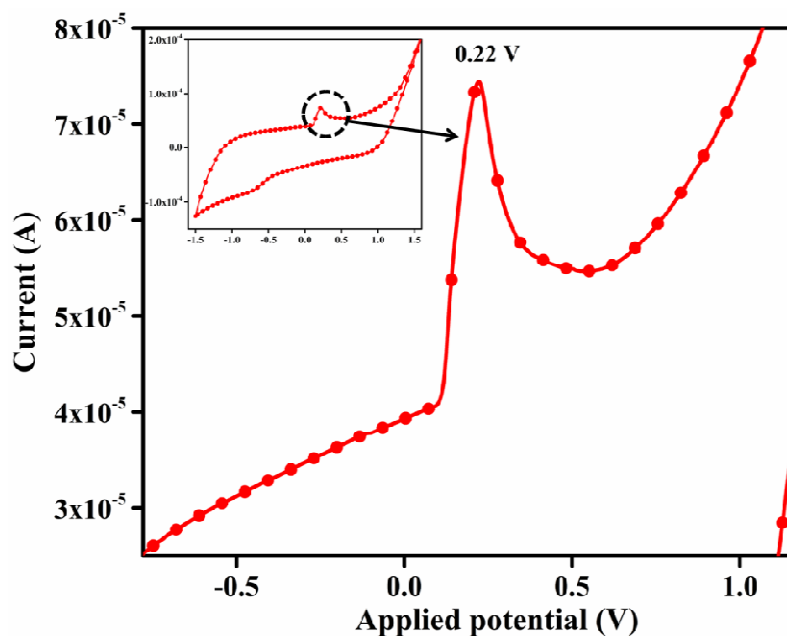


**Figure 4.1.4** Cyclic voltammogram recorded for silver nanoparticle modified SPE using 0.1 M KCl supporting electrolyte. Electrode modification was done using 0.67 mM  $\text{AgNO}_3$ , 300 s and -1.2 V potential. Ag/AgCl used as reference electrode

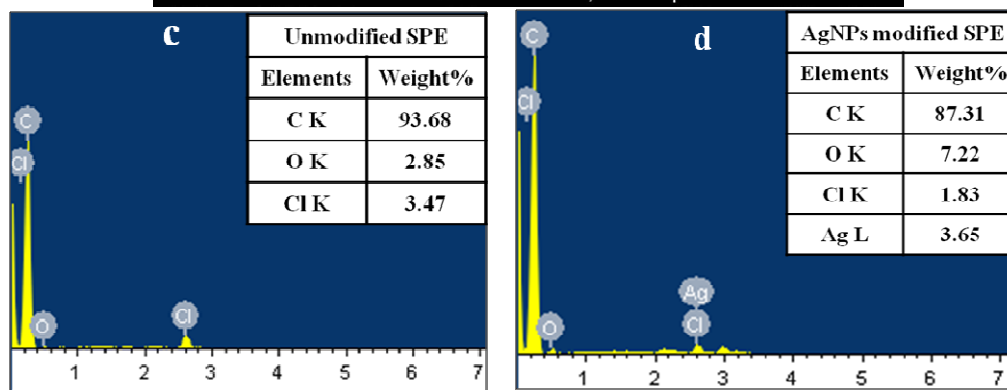
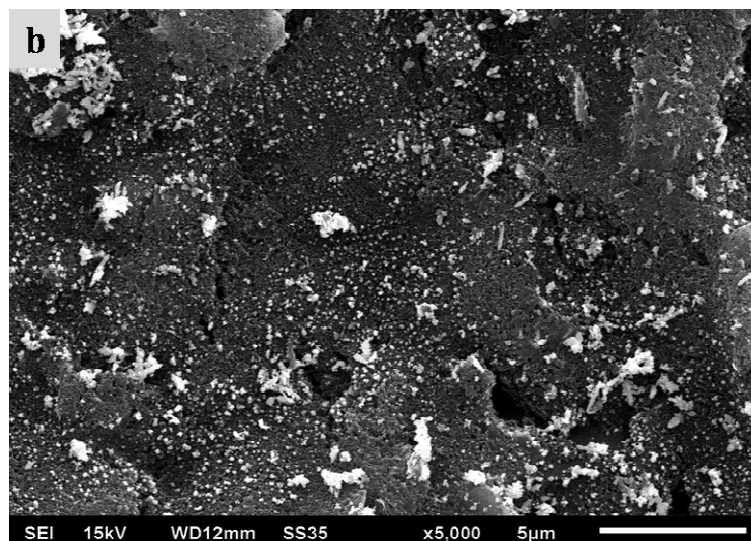
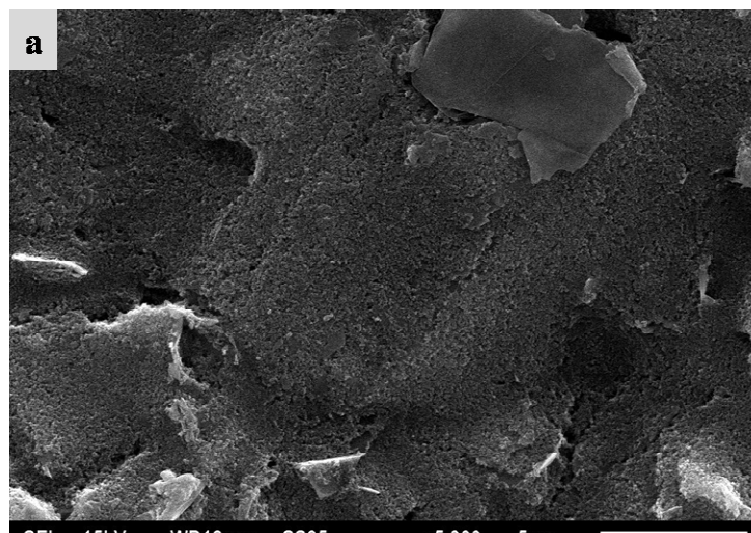


**Figure 4.1.5** SEM images observed for (a) unmodified SPE, (b) AgNPs modified and EDX analysis (c) unmodified SPE and (d) AgNPs modified SPE

## 4.2. Ion-recognition of JS-2/AgNPs modified SPE

JS-2/AgNPs modified SPE was electrochemically characterized using CV and metal ions selectivity was analyzed using DPV. Structure of JS-2 is revealed in Figure 4.2 Detailed study of the modified electrode has been discussed in this section.

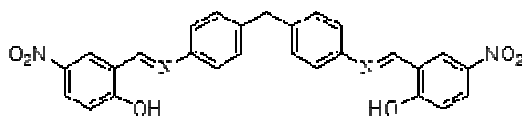


**Figure 4.2** Structure of JS-2

### 4.2.1. Selection of supporting electrolyte

Generally, supporting electrolyte has great impact on the redox signals detected for the sample. In instruction to obtain the best electrochemical response, cyclic voltammetry scan was noted using JS-2 ionophore modified with silver nanoparticles deposited SPEs (JS-2/AgNPs-SPE) in 0.1 M of various electrolytes namely  $\text{CH}_3\text{COONa}$ ,  $\text{NaOH}$ ,  $\text{NH}_4\text{Cl}$  and  $\text{KCl}$ . All the electrolytes taken were of 0.1 M concentration. It can be noted from Figure 4.2.1 that distinguished sharp peaks with noticeable current magnitude was obtained in  $\text{KCl}$  (0.1 M). Probable reason for this can be explained on the basis of solid-state nature of SPE. Silver/silver chloride reference electrode present on the polyester substrate does not have any internal solution. So, for the proper working of electrode, concentration of chloride in the electrolyte medium must be preserved. An anodic peak corresponding to AgNPs was observed in every medium, while cathodic peaks at 0.68 V and -0.9 V indicate the presence of ionophore. The cathodic peak attributed the imine bond reduction present in cavity of JS-2. Hence,  $\text{KCl}$  (0.1 M) had been selected as electrolyte medium for further revisions.

### 4.2.2. Electrochemical response of JS-2/AgNPs modified SPE

An electrochemical response of JS-2/AgNPs modified SPE was obtained using cyclic voltammetry and compared with the redox characteristics with original SPE. A comparative cyclic voltammogram of unmodified SPE and JS-2/AgNPs modified SPE was recorded in  $\text{KCl}$  (0.1 M) as supporting electrolyte in full potential range (+2.0 V to -2.0 V) at scan rate  $50 \text{ mV s}^{-1}$  shown in Figure 4.2.2.A In case of unmodified SPE, no redox peaks were observed because there was no electro-active material present in the

working electrode surface. Further, in comparison to plain SPE, JS-2/AgNPs modified SPE showed distinguished reduction peaks. The reduction peak observed at 0.65 V in cyclic voltammograms attributed for the imine double bond reduction to amine.

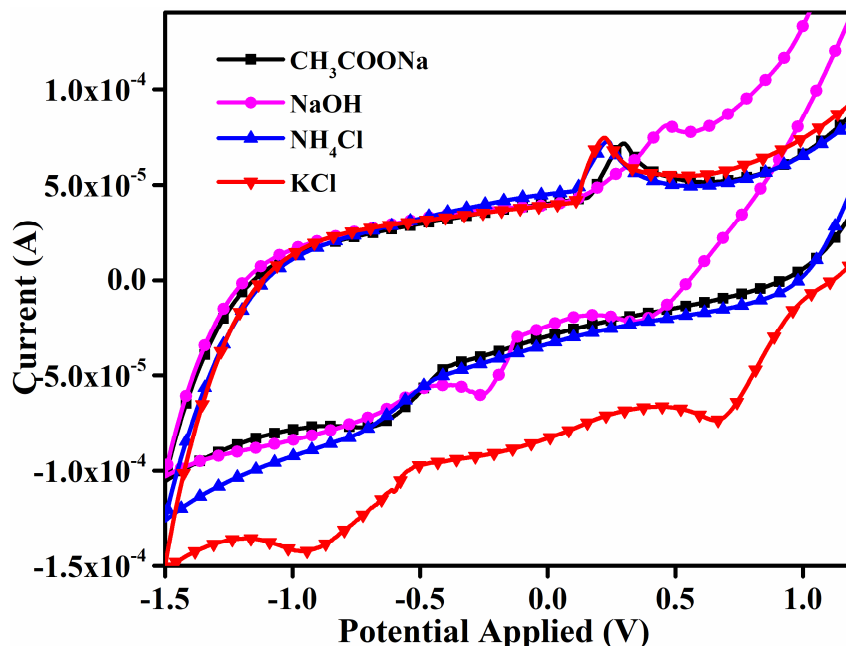


**Figure 4.2.2.A** Cyclic voltammograms recorded on JS-2/AgNPs modified SPE using different electrolytes,  $\text{CH}_3\text{COONa}$ ,  $\text{NaOH}$ ,  $\text{NH}_4\text{Cl}$  and  $\text{KCl}$  (0.1 M). Scan rate used was  $50 \text{ mV s}^{-1}$  and  $\text{Ag}/\text{AgCl}$  was used as reference electrode

Nature of substituents around aromatic groups existence on any side of the imine group influence the reduction potential of Schiff base.<sup>85</sup> Nitro group ( $-\text{NO}_2$ ) plays a vital role in reduction, because of its electron withdrawing nature. Moreover, existence of nitro group ( $-\text{NO}_2$ ) at para position with respect to hydroxyl group in JS-2 enhances the Lewis acidity of OH, which eventually favors the reduction of unsaturated to saturated amine.<sup>86</sup>

Furthermore, surface of working electrodes was also analyzed using scanning electron microscopy (SEM) and EDX analysis shown in Figure 4.2.2.B. As observed in SEM image, surface of the JS-2/AgNPs has been modified because of which surface appears to be porous and uneven therefore, fast electron transfer takes place on the surface.

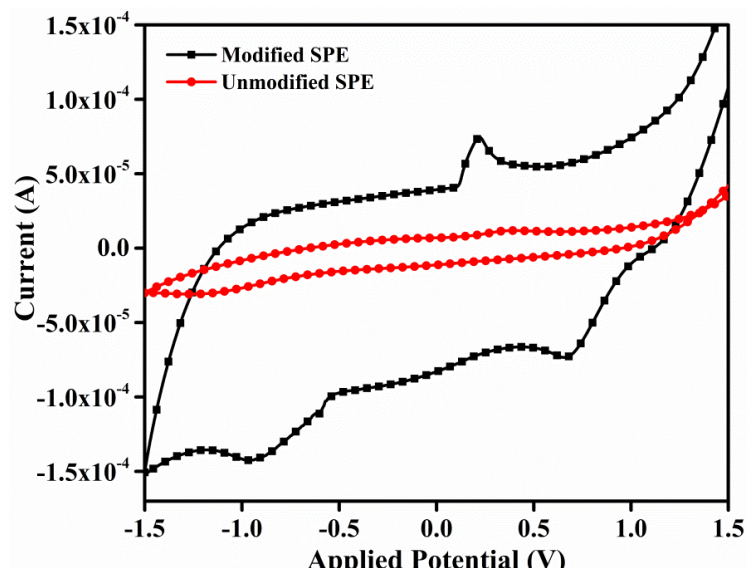


**Figure 4.2.2.B** Cyclicvoltammograms of unmodified and modified SPE recorded in KCl (0.1 M) supporting electrolyte using  $50 \text{ mV s}^{-1}$  scan rate

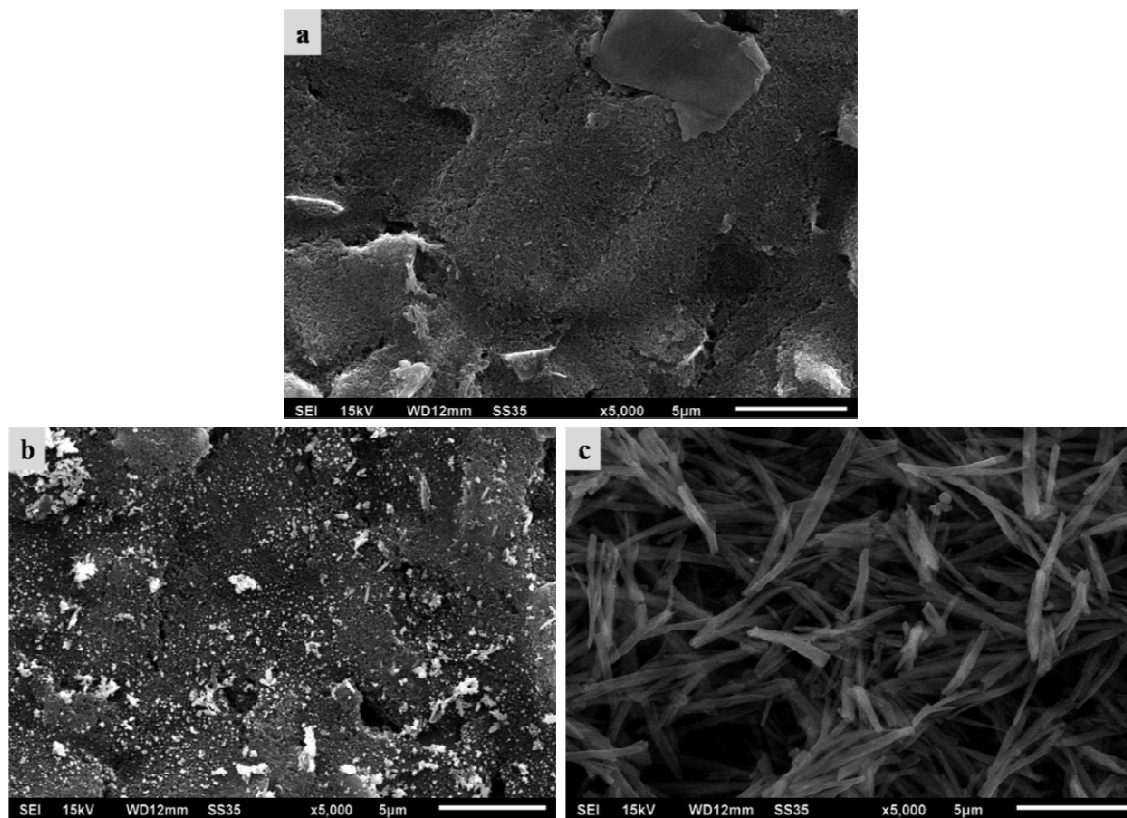


**Figure 4.2.2.C** SEM analysis of (a) Unmodified working electrode, (b) AgNPs modified working electrode and (c) JS-2/AgNPs modified working electrode of SPE

### 4.2.3. Impact of Scan Rate

Impact of scan rate on the potential and current of cathodic peak was studied by cyclic voltammetry performed on JS-2/AgNPs modified SPE at various scan rates. Cyclic voltammograms were noted in the range of 20-160 mVs<sup>-1</sup> using KCl (0.1 M), as supporting electrolyte and presented in Figure 4.2.3 (A). It can be noted that peak current had been increased with an increase of scan rate value 20 mV s<sup>-1</sup> to 160 mV s<sup>-1</sup>. Cathodic peak current was linearly depending upon square root of scan rate ( $v^{1/2}$ ) which indicated that this is in accordance with Randle–Sevcik equation (1).

$$i_p = (2.69 \times 10^5) n^{3/2} A D^{1/2} C v^{1/2} \quad (1)$$

where,  $i_p$  = peak current at redox potential,  $n$  = number of electrons transferred during redox events occurring at electrode surface,  $A$  = surface area of electrode (cm<sup>2</sup>),  $C$  = concentration of the electro active species (mol cm<sup>-3</sup>) and  $D$  = diffusion coefficient (cm<sup>2</sup> s<sup>-1</sup>) and  $v$  is scan rate (V s<sup>-1</sup>)<sup>87</sup>

Regression equation obtained from linear plot drawn between peak current verses  $v^{1/2}$  is presented as  $I_{pa}=1.48E-5x-1.88E-5$  and  $I_{pc}=-1.96E-5x-1.96E-5$ , where (Y: peak current/A and x: square root of scan rate/mV s<sup>-1</sup>). Also, correlation coefficient ( $R^2$ ) values for both reduction and oxidation processes were obtained as 0.94 and 0.99 showing that diffusion controlled reaction took place over the surface of working electrode. Furthermore, the peak potential value was not exaggerated by the change in scan rate. This shows that reversible reaction occurred at the electrode surface. Thus, overall reversible process was controlled by diffusion of electrons at electrode surface.

### 4.2.4. Influence of presence of different ions

Being a more sensitive voltammetric technique differential pulse voltammetry (DPV) was used to explore metal ion recognition ability of J-2/AgNPs modified SPE. Distinct peaks were observed in the potential range of 0.0 V to 1.5 V. Best response was achieved with scan rate of 50 mV s<sup>-1</sup>

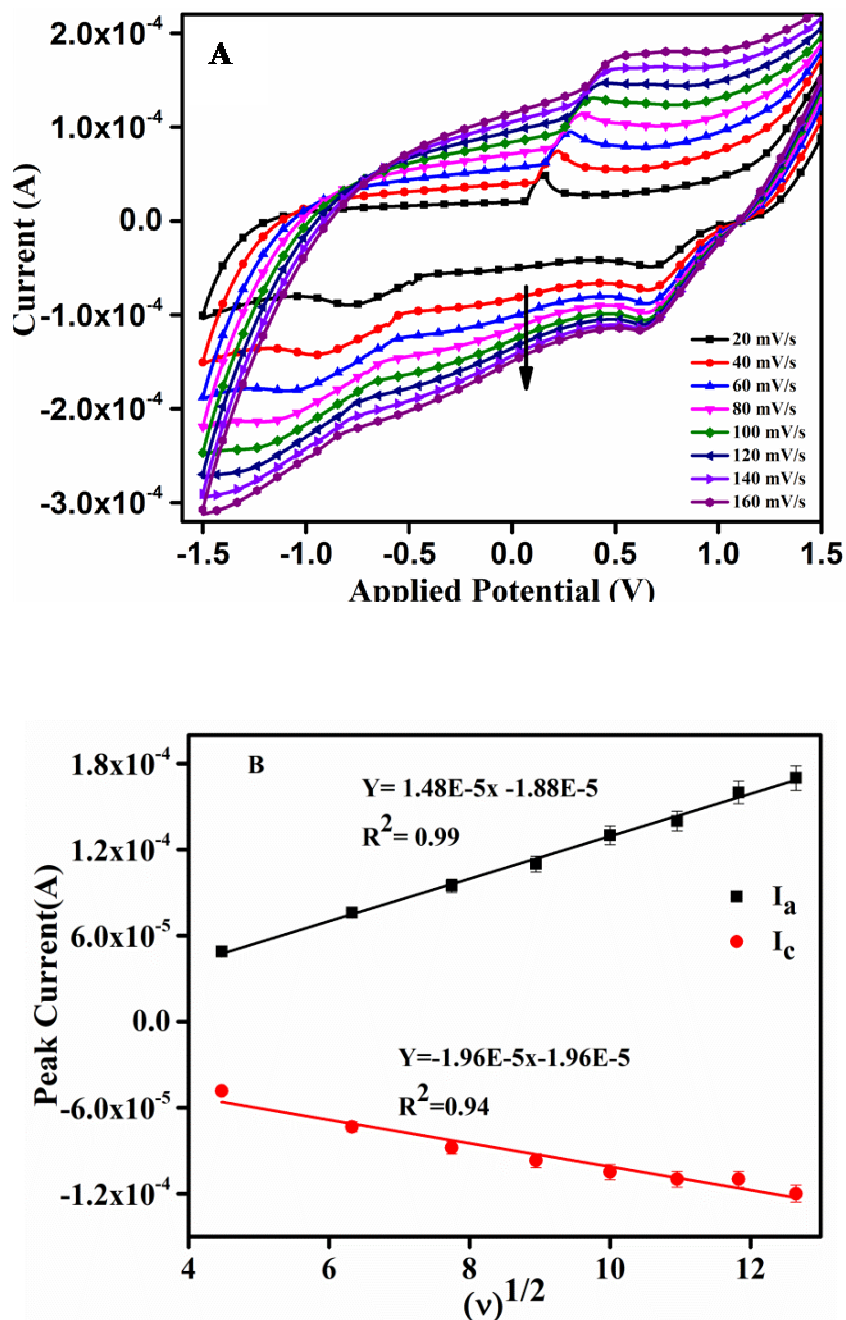


**Figure 4.2.3(A)** Cyclic voltammograms recorded on JS-2/AgNPs modified SPE at different scan rates from 20 mV s<sup>-1</sup> to 160 mV s<sup>-1</sup>. **(B)** Linear plots between peak current and square root of scan rate ( $v^{1/2}$ ) corresponding graph A, recorded using KCl (0.1 M) as electrolyte and Ag/AgCl as a reference electrolyte

Electrochemical selectivity of the SPE was enhanced after modification. It was measured that occurrence of ionophore in the modified electrode surface might provide metal-ion recognition ability to the proposed sensor. Experimental importance of voltammetry is due to its efficiency for detection of metal ions which can have strong binding with ionophore to be studied. Therefore, using optimized parameters selectivity of the electrochemical probe was explored by conducting DPV studies in the existence of altered ions. Modification in peak potential and current magnitude with respect to the values originally on modified electrode (assigned to ionophore) was observed. In the existence of various analytes such Li (I), Mg (II), Na (I), K (I),Ca (II), Cu (II),Cr (III), Al (III), Fe (II), Co (II), Ni (II),Zn (II),Pb (II) change in redox behavior of proposed electrode was detected and experiments were conducted in KCl (0.1 M) electrolyte. It was observed that a new cathodic peak at 0.2 V was observed along with shift of cathodic peak potential from 8.6 V to 9.6 V in the appearance of Fe (II), as observed in Figure 4.2.4. Whereas, other metal ion did not impart significant change on redox signals of the ligand apart from insignificant change in peak current values and results were arranged in Table 4.2.

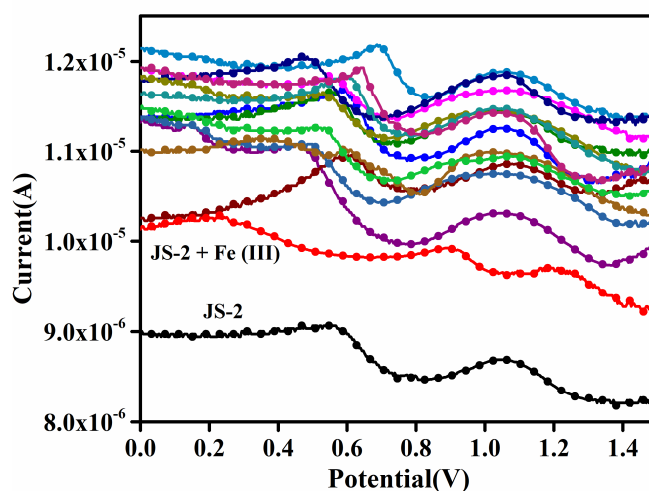


**Figure 4.2.4** Differential pulse voltammograms of JS-2/AgNPs modified SPE showing cathodic scan in the presence of different metal ions, Li (I), Na (I), Mg (II), K (I),Ca (II), Cr (III), Al (III), Fe (II), Co (II), Ni (II),Cu (II),Zn (II), Pb (II) recorded using KCl (0.1 M) as supporting electrolyte in the potential range from +1.5 V to -0.1 V

**Table 4.2.1** Voltammetric peak potential values for the ionophore JS-2 and metal receptor complexes with various metal ions

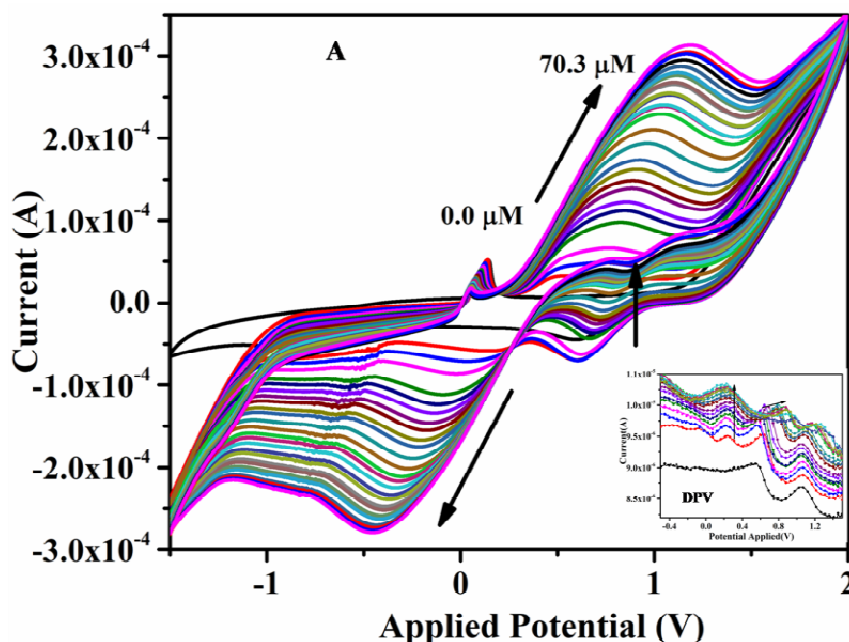
Metal ions	Cathodic peak potential		Shift in peak potential	
	$E_{p1}$	$E_{p2}$	$\Delta E_{p1}$	$\Delta E_{p2}$
Ligand	0.57	1.06		
Li (I)	0.47	1.05	-0.1	-0.01
Na (II)	0.49	1.07	-0.08	0.01
Mg(II)	0.54	1.05	-0.03	-0.01
K (I)	0.53	1.05	-0.04	-0.01
Ca (II)	0.58	1.06	0.01	0.0
Cr(III)	0.55	1.06	-0.02	0.0
Al (III)	0.68	1.06	0.11	0.0
Co (II)	0.57	1.07	0.0	0.01
Ni (II)	0.61	1.06	0.04	0.0
Cu(I)	0.48	1.06	-0.09	0.0
Zn (II)	0.64	1.05	0.07	-0.01
Pb (II)	0.61	1.05	0.04	-0.01
Fe (II)	0.22	1.24	-0.35	0.18

#### 4.2.5. Quantitative measurement of Fe (II) using SPE

Under optimal conditions for JS-2/AgNPs modified SPE (0.1 M KCl), differential pulse voltammetric study was done for reduction of imine to amine at different concentrations. Linear response range exposed by projected sensor was from 0.0  $\mu\text{M}$  to 70.3 $\mu\text{M}$  with the limit of detection 0.19  $\mu\text{M}$ . This shows that the existence of ferrous content in real life samples with the limit of detection 0.19  $\mu\text{M}$  can be detected using the prepared JS-2/AgNPs modified sensor.

The linear graph is  $y = 4.89x + 7.056E-6$  (y: peak current/ $\mu\text{A}$  and x: concentration of Fe (III)/ $\mu\text{g L}^{-1}$ ) with correlation coefficient  $R^2 = 0.99$ . Limit of Detection (LOD) was calculated using formula  $3\sigma/m$ ;

$\sigma$  = standard deviation of the blank (estimated by five replicate determination of the blank signals),  $m$  = slope of calibration graph (Bard)



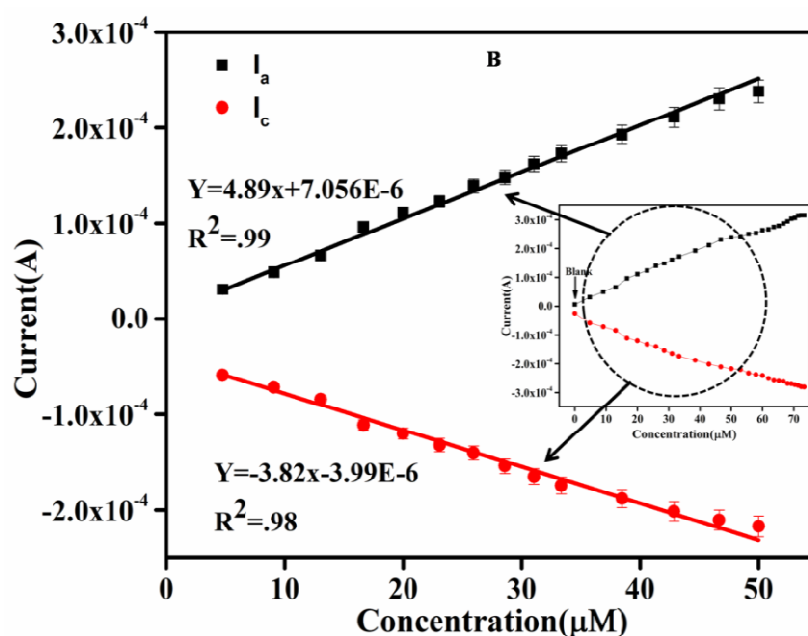


**Figure 4.2.5** (A) Cyclic voltammograms of JS-2/AgNPs modified electrode in presence of different concentrations of Fe (II) in the concentration range of 0.0  $\mu\text{M}$  to 70.3  $\mu\text{M}$  using KCl (0.1 M) as electrolyte and Ag/AgCl as a reference electrode. (B): Linear plots between current and analyte concentration corresponding graph A using KCl (0.1M) as supporting electrolyte

#### 4.2.6. Interference study

For any sensor, the most prominent characteristic is its selectivity. This is a significant factor as it tells us about its nature and amount which can be used for the detection of specific metal ion in an existence of the other intrusive ions. By the means of cyclic voltmmrtery, peak current of JS-2/AgNPs modified screen printed electrode was optimized in the presence of interfering cations and anions like Ca (II), Li (I), Na (I), Mg (II), Cu (II), K (I), Cr (III), Al (III), Fe (II), Co (II), Zn (II), Ni (II),Hg (II) and Pb (II) was studied. A 10  $\mu\text{L}$ mixture of equivalent amount of Fe (II) ion with interfering ions is prepared and was dispensed on the modified JS-2/AgNPs by drop coating on 30  $\mu\text{L}$  solution of supporting electrolyte KCl (0.1M). Cathodic peak current was optimized. As such no major displacement was observed in presence of other ions on the modified SPE. Percentage of change in peak current is given in Table 4.2.2, which was reported below 10% .That means there is good selectivity of Fe (II) in our proposed sensor.

**Table 4.2.2** Table showing reduction peak % current of JS-2•Fe (II) complex in presence of various interfering ions

<b>Interfering Ions (<math>10^{-2}</math> M*)</b>	<b>Change of peak current (%)</b>
Na (I)	-4.85
Li (I)	-0.65
K (I)	+6.53
Mg (II)	+1.83
Ca (II)	+4.14
Cr (III)	+2.61
Al (III)	+5.39
Fe (II)	+7.50
Co (II)	+4.77
Ni (II)	+6.03
Cu (II)	+3.18
Zn (II)	+6.41
Hg (II)	+1.80
Pb (II)	+5.62

#### 4.2.7. Real life sample study

For real life sampling, Fe (II) was detected in wheat samples and black tea samples using JS-2/AgNPs modified SPE. Wheat sample was prepared by adding nitric acid (50 mL, 2.0 M) into powdered wheat seeds (0.5 g) and for 15 minutes mixture was ultrasonicated. For neutralization purpose NaOH (1.0 M) and as a reducing agent hydrazine sulphate solution (2 mL, 0.01 M) was added. Filtration and dilution was done with distilled water (100 mL) for detection of Fe (II) ions from sample.

Second sample i.e., black tea sample was prepared using reported method.<sup>88</sup> In a 10 mL beaker a black tea sample (1 g) was weighed. Further, adding nitric acid (10 mL, 2 mol L<sup>-1</sup>) and perchloric acid (4 mL, 0.1 mol L<sup>-1</sup>) into sample solution monitored by absorption on a heating plate placed in fuming hood. Afterwards, NaOH (1 mol L<sup>-1</sup>) was further added for neutralization and as a reducing agent hydrazine (1 mL, 0.01 mol L<sup>-1</sup>) was added to the solution. Using 100 mL distilled water, filtration and dilution process was being completed. Then iron content present in the black tea was detected using the modified electrode and the data was further confirmed with Atomic Absorption Spectroscopy (AAS). Table 4.2.3 showing the results found from four replicate measurements. Obtained data is in noble agreement between results obtained using the proposed sensor and AAS.

**Table 4.2.3** Measurement of Fe (II) in real life samples using proposed voltammetric sensor and compared with AAS method

S.No	Sample	Amount of Fe (II) in mg/L ( $\pm$ SD)	
		Proposed voltammetric method	AAS method
1.	Wheat sample	0.26 ( $\pm$ 0.05)	0.30 ( $\pm$ 0.06)
2.	Black tea	0.67 ( $\pm$ 0.04)	0.69 ( $\pm$ 0.06)

#### 4.2.8. Conclusions

Fe (II) ions, investigated electrochemically by cyclic voltammetry using JS-2/AgNPs modified screen printed carbon paste electrode. Electrochemical features of fabricated electrode gives sharp peaks corresponding to KCl (0.1 M), as a supporting electrolyte. Prepared electrode is highly sensitive towards Fe (II) in the range of concentration (0.0  $\mu\text{M}$  to 70.3 $\mu\text{M}$ ) with detection limit of 0.19  $\mu\text{M}$ . No interference with other metal ions being noticed and SPE can be recycled after treating with EDTA solution (0.1 M). This fabricated sensor can be used for on-site recognition.

#### 4.3. Ion-recognition of JS-3/AgNPs

Redox characteristics of JS-3/AgNPs modified SPE was carried out using CV and DPV. Several parameters like supporting electrolyte, scan rate were optimized before carrying out sensing activity. Chemical structure of JS-3 ionophore is shown in Figure 4.3. Electrochemical studies of the JS-3/AgNPs modified electrodes have been discussed in detail.

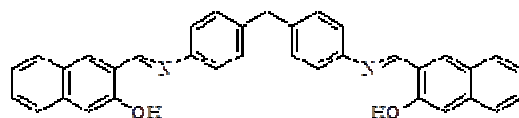


**Figure 4.3:** Structure of JS-3

##### 4.3.1. Supporting electrolyte selection

The influence of the presence of supporting electrolyte on the redox character of JS-3/AgNPs modified SPE was also determined using CV. As explained in previous section well defined behavior of the voltammogram was obtained in KCl (0.1 M). Hence, KCl(0.1 M) was preferred as an experimental solution for carry out further experiments.

##### 4.3.2. Study of surface of bare and modified SPE

Extent of sensing is purely based upon surface activity of the working electrode. In that reference, for making surface of working electrode a better sensor, electrode was modified with silver nanoparticle and schiff base derivative. Further, modified surface has been analyzed using surface analysis technique such as Energy Dispersive X-Ray

Spectroscopy(EDX) and scanning electron microscopy (SEM), which provided more information about surface morphology and composition of unmodified and modified SPE as shown in Figure 4.3.2(A).

SPE was initially modified using silver nanoparticles (deposited electrochemically) on the working electrode by performing chronoamperometric at potential of -1.2 V for 300 seconds. With deposition of silver nanoparticles, white particles were observed at the surface of SPE. EDX data also confirmed the presence Ag at the surface of AgNPs modified electrode. Further, Schiff base was deposited on the modified electrode using drop coating method. Schiff base ionophore strongly absorbed on the rough surface of Ag deposited SPE and redox reactions took place at the surface was studied by differential pulse voltammetry and cyclic voltammetry. An evaluation of bare and modified SPE was performed electrochemically on the surface working electrode with supporting electrolyte KCl (0.1M) in the full range of potential +2.0 V to -2.0 V at 50 mVs<sup>-1</sup> scan rates. In case of electrode without modification no redox peaks were observed as there was no electro-active compound on the working electrode surface whereas, in case of electrode with JS-3/AgNPs modification, two cathodic peaks were noticed at 0.55 V and -0.8 V in CV. Clearly visible in Figure 4.3.2(B).

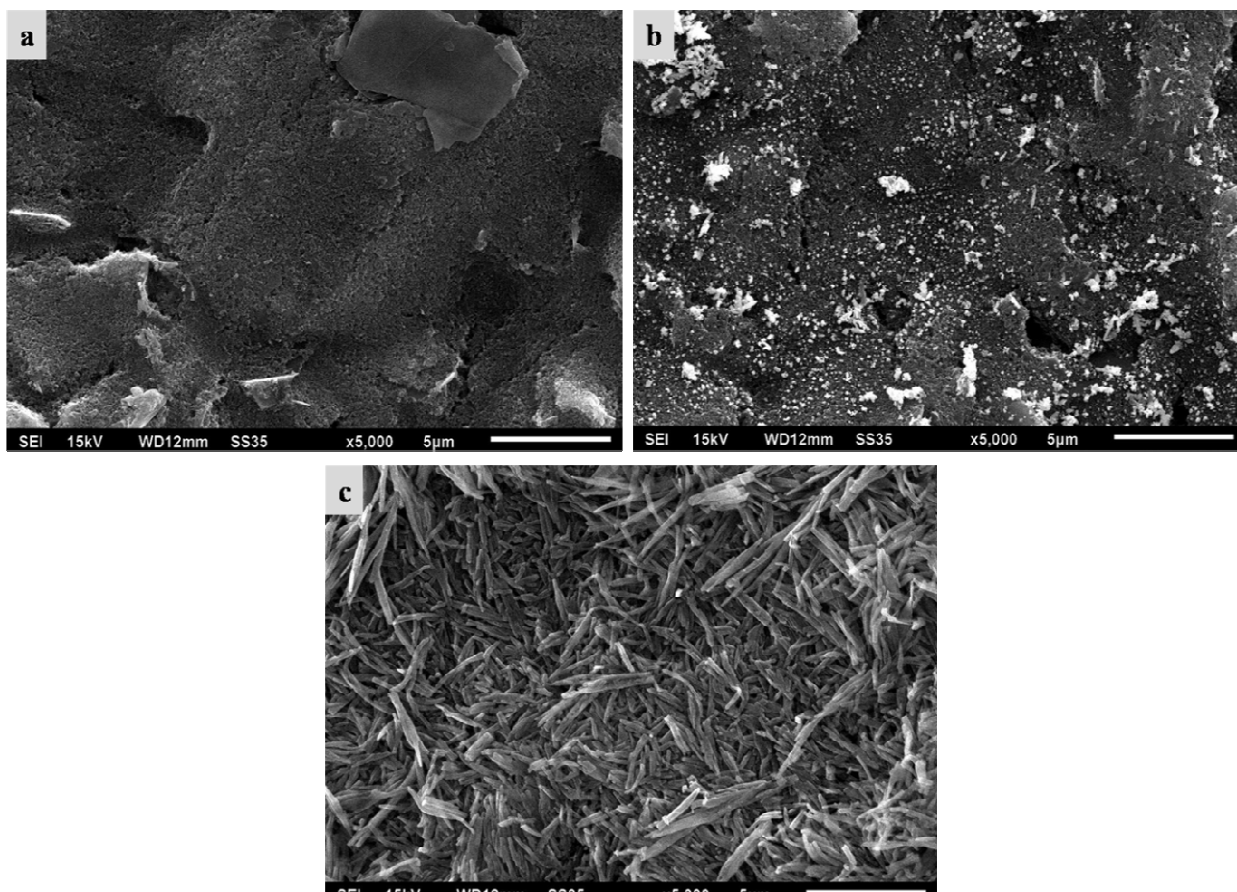


**Figure 4.3.2** SEM images of (a) bare working electrode, (b) AgNPs modified electrode and (c) JS-3/AgNPs modified electrode

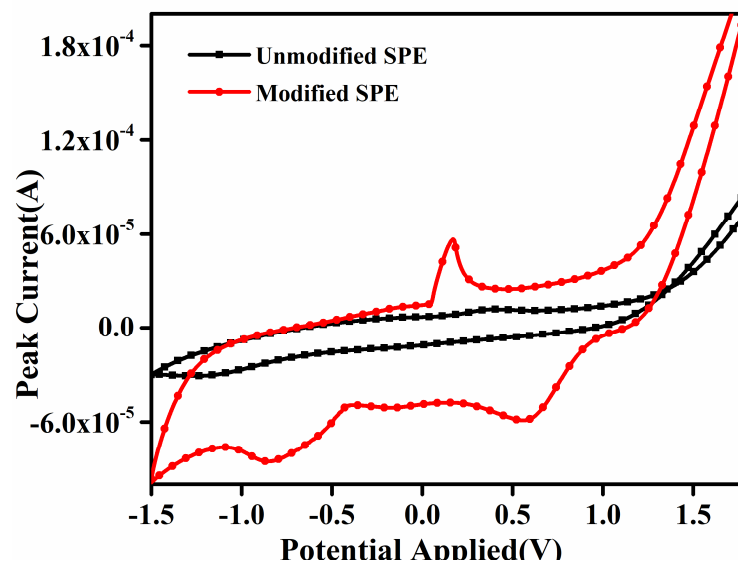


**Figure 4.3.3** Assessment of the cyclic voltammograms of bare and modified JS-3/AgNPs modified SPE measuring in the potential range of the -1.5 to 1.5 V using KCl (0.1 M) with scan rate 50 mVs<sup>-1</sup>

#### 4.3.3. Effect of scan rate on cathodic peak current

Some useful information has been collected by analyzing the electrochemical process that has been taken place on the surface of electrode, which can be found from relationship of peaks current with rate of scan. Thus, scan rate studies were done using cyclic voltammogram. To know whether, process taking place at the JS-3/AgNPs modified electrode was under diffusion controlled or adsorption controlled. Cyclic voltammograms were noted at different scan rates falls in the range of 20-60 mVs<sup>-1</sup> using KCl (0.1M) as supporting electrolyte and shown in figure 4.3.4 That was being observed that with the enhancement of scan rate, peak current was increasing and linear dependence co-relation was observed between peak current versus square root of scan rate ( $v^{1/2}$ ) which was specified by following Randle-Sevcik equation:

$$i_p = (2.69 \times 10^5) n^{3/2} A D^{1/2} C v^{1/2}$$

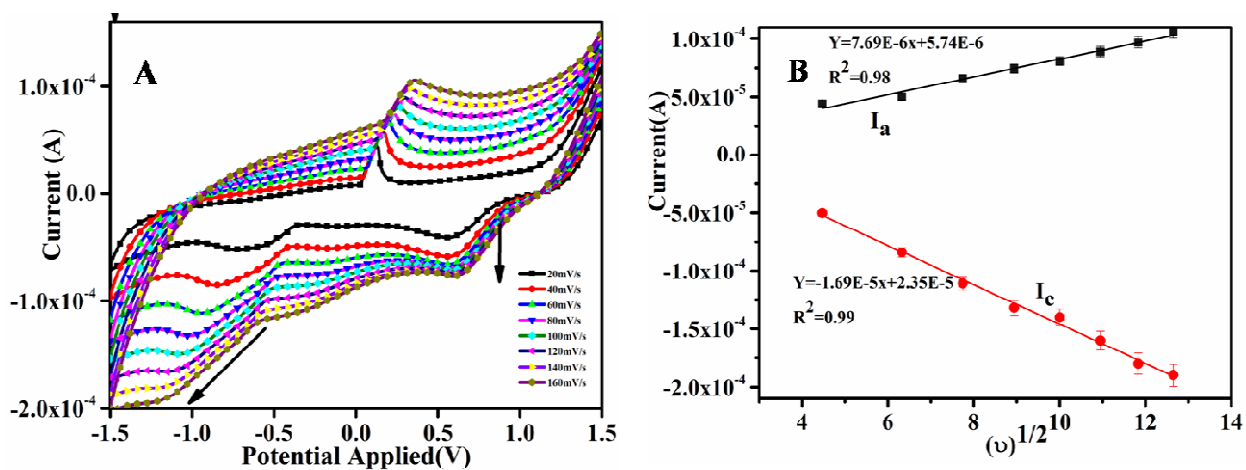
Where, n = number of electrons transferred in the redox events (generally),  $i_p$  = peak current at redox potential, C = concentration of the electro active species (mol cm<sup>-3</sup>), A = electrode surface area (cm<sup>2</sup>), D = diffusion coefficient (cm<sup>2</sup> s<sup>-1</sup>) and v = scan rate (V s<sup>-1</sup>)

The linear relationship obtained using cyclic voltammograms was analyzed and gave regression equations from anodic and cathodic peaks, respectively:

For anodic:  $Y=7.69E-6x+5.74E-6$  and

For cathodic:  $Y=1.69E-5x+2.35E-5$

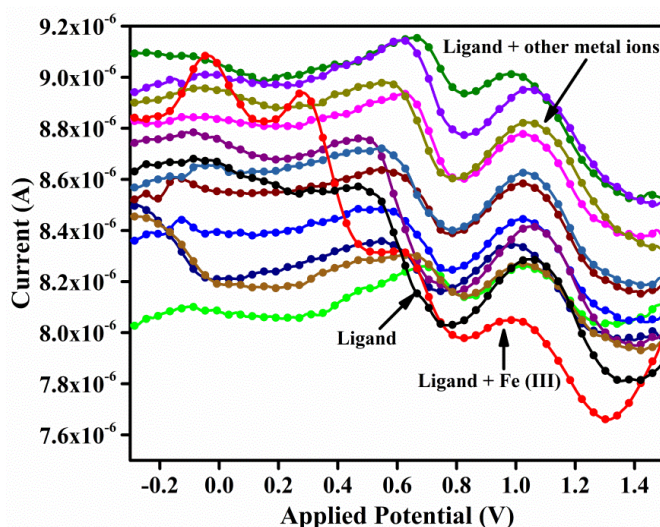
Where,  $x$ : square root of scan rate/ $mVs^{-1}$  and  $Y$ : peak current/ $A$ . Also, the correlation coefficient ( $R^2$ ) values for both anodic and cathodic peaks were observed as 0.98 and 0.99, respectively. This shows that process occurring on working electrode is reversible in nature. So, The reversible process was under control of diffusion of electrons at the surface of electrode.



**Figure 4.3.4** (A) Cyclic voltammograms recorded on JS-3/AgNPs modified SPE at different scan rates from 20  $mV s^{-1}$  to 160  $mVs^{-1}$ . (B) Linear plots between peak current and square root of scan rate ( $v^{1/2}$ ) corresponding graph A recorded using KCl (0.1 M) as electrolyte and Ag/AgCl as a reference electrolyte

#### 4.3.4. Sensing activity at the modified electrode

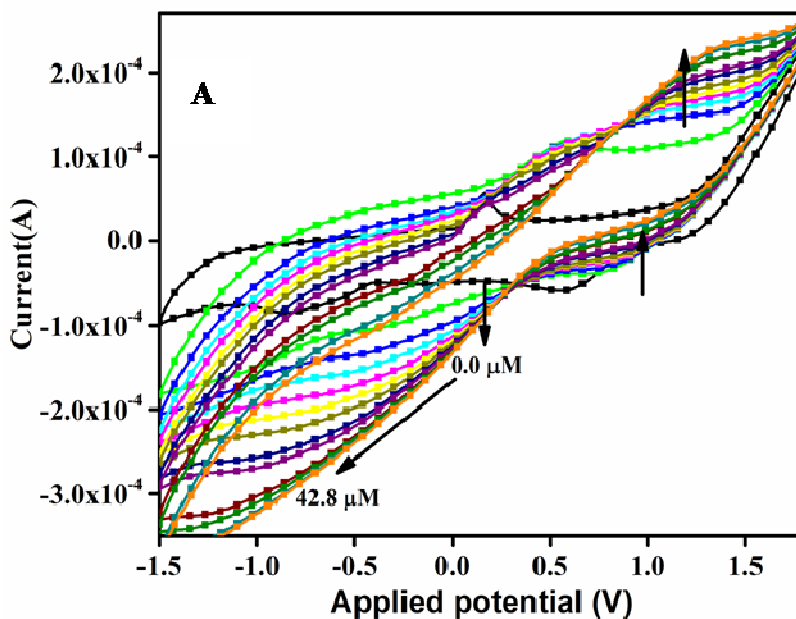
Performance of the electrochemical method was enhanced by modification of the working electrode and evaluated by different studies like metal ion sensing, interference and real life sampling. It was assumed that existence of ionophore on the silver nanoparticles modified electrode provides metal-ion recognition ability to the proposed sensor. Therefore, using some known optimized parameters selectivity of the electrode for metal ions was investigated by conducting differential pulse voltammetry. Different cations were tested for possible selectivity. Alteration, in peak current was noted with respect to the original values of the modified electrode, in the existence of various analytes such as Mg (II), K (I), Ca (II), Cr (III), Fe (II), Fe (III), Na (I), Co (II), Ni (II), Al (III), Cu (II), Li (I), and Zn (II) in KCl(0.1 M), as supporting electrolyte. One new cathodic peak was observed at 0.14V along with the shift of cathodic peak potential from 0.51 V to 0.63 V due to the presence of Fe (III), as shown in Figure 4.3.4. While other metal ions failed to show any shifting or any new peak, indicating that they were not selected with the proposed sensor.



**Figure 4.3.5** Differential pulse voltammograms of JS-3/AgNPs modified SPE showing cathodic scan in the presence of different metal ions, Li (I), Na (I), Mg (II), K (I), Ca (II), Cr (III), Al (III), Fe (II), Co (II), Ni (II), Cu (II), Zn (II), Pb (II) recorded using KCl (0.1 M) as supporting electrolyte in the potential range from +1.5 V to -0.2 V

#### 4.3.5. Detection limit of proposed sensor for Fe(III)

With the help of cyclic voltammetry technique, analytical performance of JS-3/AgNPs was evaluated. Under the optimal conditions, the CV response of different concentrations of Fe (III) ion at JS-3/AgNPs electrode was noted. The peak current consequent to the modified electrode increased with increase in the Fe (III) ion concentration. Straight line relationship was noticed between the cathodic peak current and Fe (III) ion concentration from 2.4  $\mu\text{M}$  to 37.5  $\mu\text{M}$ , while the full working range was 0.0  $\mu\text{M}$  to 42.8  $\mu\text{M}$ . The limit of detection was calculated as 1.73 $\mu\text{M}$ . This shows that the presence of Fe (III) in real life samples can be detected as low as 1.73 $\mu\text{M}$  can be detected using the proposed voltammetric sensor modified with JS-3/AgNPs.



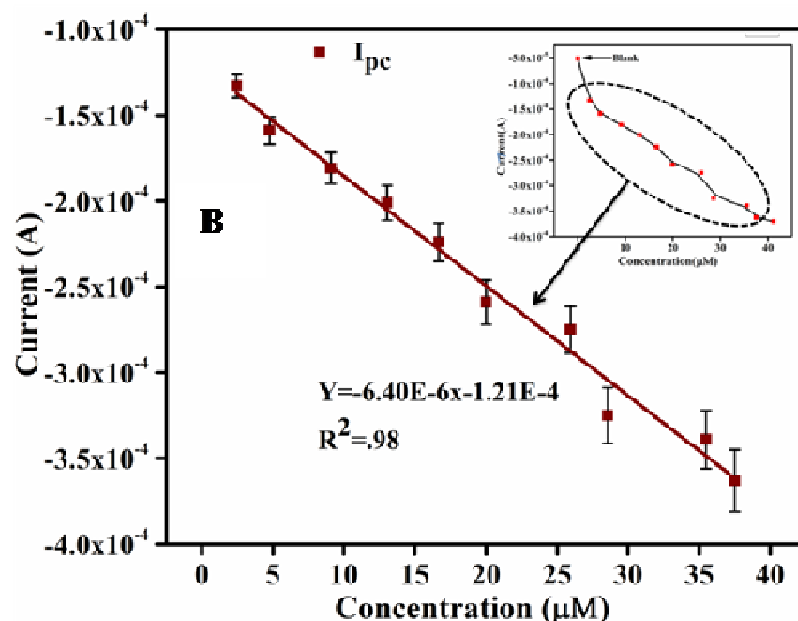


**Figure 4.3.6** (A) Cyclic voltammograms of JS-3 modified electrode in existence of different concentrations of Fe (III) in the concentration range of 0.0  $\mu\text{M}$  to 42.8  $\mu\text{M}$  using KCl (0.1 M) as electrolyte and Ag/AgCl as a reference electrode.(B)Linear plots between current and analyte concentration corresponding graph A using KCl (0.1M) as supporting electrolyte

#### 4.3.6. Interference study

After completing, the simultaneous and individual measurements of Fe (III) on the JS-3/AgNPs modified SPE, the mutual interferences between Fe (III) and other heavy metal ions like Li (I), Na (I), K (I), Ca (II), Mg (II), Cr (III), Co (II), Al (III), Fe (II), Ni (II), Cu (II), Pb (II) and Zn (II) was studied at the JS-3/AgNPs modified SPE. Signals were observed in the existence of 10-times higher concentrated secondary ions. But no significant change on the peaks was observed. All the signal values were close to each individual measurement. Change in current magnitude was recorded below 10% which is shown below in Table 4.3, so, it was concluded that the concentration of other cations did not have any influence on the signals of the Fe (III) on the modified electrode. Hence, the proposed sensor has good selectivity with Fe (III) in existence of other interfering heavy metal ions.

**Table 4.3.1** Table showing cathodic peak % current of JS-3Fe (III) complex in presence of various interfering ions

<b>Interfering Ions</b>	<b>Change of cathodic peak current (%)</b>
<b>10<sup>-2</sup> M*</b>	
Mg (II)	-1.21
Na (I)	-2.32
Li (I)	-0.99
K (I)	-0.66
Ca (II)	-0.59
Cr (III)	0.99
Al (III)	1.21
Co (II)	-0.66
Cu (II)	1.76
Ni (II)	-0.44
Zn (II)	0.44

#### **4.3.7. Real Life Sampling**

For real life sampling, Fe (III) was detected in water sample using JS-3/AgNPs modified SPE. Filtration of the sample was done over 0.45 mm membrane filter and centrifuged at the rate of 5000 rpm for removing impurities. Further, sample was oxidized in the presence of concentrated acid HNO<sub>3</sub> and 1% H<sub>2</sub>O<sub>2</sub>. The solution was kept at 3 pH and diluted with distilled water in a 100 mL conical flask. Fe (III) was detected in water

samples and confirmed with Atomic Absorption Spectroscopy (AAS). These results attained from five repetitions extents are set in Table 4.2.3. Obtained data is in good agreement between the proposed sensor and AAS.

**Table 4.3.2** Table showing data recorded for real-life samples using proposed sensor and verified with AAS

S.No	Sample	Amount of Fe (II) in mg/L ( $\pm$ SD)	
		Proposed voltammetric method	AAS method
1.	Water sample	0.28 ( $\pm$ 0.05)	0.33 ( $\pm$ 0.06)

#### 4.3.8. Conclusions

Electrochemically, Fe (III) ions were investigated by cyclic voltammetry using JS-3/AgNPs modified screen printed carbon paste electrode. Electrochemical behaviour of fabricated electrode exhibited sharp peaks for the ionophore JS-3 in KCl (0.1 M), as a supporting electrolyte. The proposed electrode is highly sensitive for Fe (III) in the range of concentration (0.0  $\mu$ M to 42.8  $\mu$ M) with detection limit 1.73  $\mu$ M. No interference with other metal ions was noticed. This sensor can further be used for the on-site detection of Fe (III) in real life samples.

## References

1. Hulanicki, A.; Glab, S.; Ingman, F., Chemical sensors: definitions and classification. *Pure and Applied Chemistry* **1991**,*63* (9), 1247-1250.
2. Brett, C.; Oliveira Brett, A. M., *Electrochemistry: principles, methods, and applications*. 1993.
3. Rudolph, M.; Reddy, D. P.; Feldberg, S. W., A simulator for cyclic voltammetric responses. *Analytical chemistry* **1994**,*66* (10), 589A-600A.
4. Compton, R. G.; Banks, C. E., *Understanding voltammetry*. World Scientific: 2011.
5. Gilman, S., The anodic film on platinum electrodes. Marcel Dekker, Inc.: New York, NY, USA: 1967; Vol. 2, pp 112-189.
6. Kerman, K.; Saito, M.; Tamiya, E.; Yamamura, S.; Takamura, Y., Nanomaterial-based electrochemical biosensors for medical applications. *TrAC Trends in Analytical Chemistry* **2008**,*27* (7), 585-592.
7. Yi, F. Y.; Chen, D.; Wu, M. K.; Han, L.; Jiang, H. L., Chemical sensors based on metal-organic frameworks. *ChemPlusChem* **2016**,*81* (8), 675-690.
8. Safin, D. A.; Babashkina, M. G.; Garcia, Y., Crown ether-containing Schiff base as a highly efficient “turn-on” fluorescent sensor for determination and separation of Zn<sup>2+</sup> in water. *Dalton Transactions* **2013**,*42* (6), 1969-1972.
9. Hassine, C. B. A.; Brourou, M.; Barhoumi, H.; Jaffrezic, N., Copper (II) Electrochemical Sensor based on Aluminon as chelating ionophore. *IEEE Sensors Journal* **2019**.
10. Kaur, H.; Singh, N.; Kaur, N.; Jang, D. O., Nano-aggregate-Fe<sup>3+</sup> complex based on benzimidazole-modified calix [4] arene for amplified fluorescence detection of ADP in aqueous media. *Sensors and Actuators B: Chemical* **2019**,*284*, 193-201.
11. Gohil, H.; Chatterjee, S.; Yadav, S.; Suresh, E.; Paital, A. R., An Ionophore for High Lithium Loading and Selective Capture from Brine. *Inorganic chemistry* **2019**.
12. Chen, W.; Ji, D.; Zhang, Y.; Xu, P.; Gao, X.; Fang, J.; Li, X.; Feng, L.; Wen, W., Schiff-base reaction induced selective sensing of trace dopamine based on a Pt<sub>41</sub>Rh<sub>59</sub> alloy/ZIF-90 nanocomposite. *Nanotechnology* **2019**,*30* (33), 335708.

13. Asadian, E.; Ghalkhani, M.; Shahrokhian, S., Electrochemical Sensing Based on Carbon Nanoparticles: A Review. *Sensors and Actuators B: Chemical* **2019**.
14. Gupta, V. K.; Mergu, N.; Kumawat, L. K.; Singh, A. K., Selective naked-eye detection of magnesium (II) ions using a coumarin-derived fluorescent probe. *Sensors and Actuators B: Chemical* **2015**,*207*, 216-223.
15. Cayuela, A.; Soriano, M. L.; Kennedy, S. R.; Steed, J.; Valcárcel, M., Fluorescent carbon quantum dot hydrogels for direct determination of silver ions. *Talanta* **2016**,*151*, 100-105.
16. Niu, W.-J.; Shan, D.; Zhu, R.-H.; Deng, S.-Y.; Cosnier, S.; Zhang, X.-J., Dumbbell-shaped carbon quantum dots/AuNCs nanohybrid as an efficient ratiometric fluorescent probe for sensing cadmium (II) ions and l-ascorbic acid. *Carbon* **2016**,*96*, 1034-1042.
17. Xie, H.; Dong, J.; Duan, J.; Waterhouse, G. I.; Hou, J.; Ai, S., Visual and ratiometric fluorescence detection of Hg<sup>2+</sup> based on a dual-emission carbon dots-gold nanoclusters nanohybrid. *Sensors and Actuators B: Chemical* **2018**,*259*, 1082-1089.
18. Yue, X.-l.; Wang, Z.-q.; Li, C.-r.; Yang, Z.-y., Naphthalene-derived Al<sup>3+</sup>-selective fluorescent chemosensor based on PET and ESIPT in aqueous solution. *Tetrahedron letters* **2017**,*58* (48), 4532-4537.
19. Kim, D. H.; Im, Y. S.; Kim, H.; Kim, C., Solvent-dependent selective fluorescence sensing of Al<sup>3+</sup> and Zn<sup>2+</sup> using a single Schiff base. *Inorganic Chemistry Communications* **2014**,*45*, 15-19.
20. Qin, J.-c.; Fan, L.; Li, T.-r.; Yang, Z.-y., Recognition of Al<sup>3+</sup> and Zn<sup>2+</sup> using a single Schiff-base in aqueous media. *Synthetic Metals* **2015**,*199*, 179-186.
21. Li, X.-B.; Chen, J.-Y.; Wang, E.-J., A Highly Selective and Sensitive Chemosensor for Colorimetric and Fluorescent Detection of Al<sup>3+</sup> and Living Cell Imaging. *Australian Journal of Chemistry* **2015**,*68* (1), 156-160.
22. Yuan, C.; Liu, X.; Wu, Y.; Lu, L.; Zhu, M., A triazole Schiff base-based selective and sensitive fluorescent probe for Zn<sup>2+</sup>: A combined experimental and theoretical study. *Spectrochimica Acta Part A: Molecular and Biomolecular Spectroscopy* **2016**,*154*, 215-219.

23. Tang, X.; Han, J.; Wang, Y.; Ni, L.; Bao, X.; Wang, L.; Zhang, W., A multifunctional Schiff base as a fluorescence sensor for Fe<sup>3+</sup> and Zn<sup>2+</sup> ions, and a colorimetric sensor for Cu<sup>2+</sup> and applications. *Spectrochimica Acta Part A: Molecular and Biomolecular Spectroscopy* **2017**,*173*, 721-726.
24. Liu, H.; Liu, T.; Li, J.; Zhang, Y.; Li, J.; Song, J.; Qu, J.; Wong, W.-Y., A simple Schiff base as dual-responsive fluorescent sensor for bioimaging recognition of Zn<sup>2+</sup> and Al<sup>3+</sup> in living cells. *Journal of Materials Chemistry B* **2018**,*6* (34), 5435-5442.
25. Wang, Y.; Ma, Z.-Y.; Zhang, D.-L.; Deng, J.-L.; Chen, X.; Xie, C.-Z.; Qiao, X.; Li, Q.-Z.; Xu, J.-Y., Highly selective and sensitive turn-on fluorescent sensor for detection of Al<sup>3+</sup> based on quinoline-base Schiff base. *Spectrochimica Acta Part A: Molecular and Biomolecular Spectroscopy* **2018**,*195*, 157-164.
26. Zhu, X.; Duan, Y.; Li, P.; Fan, H.; Han, T.; Huang, X., A highly selective and instantaneously responsive Schiff base fluorescent sensor for the “turn-off” detection of iron (iii), iron (ii), and copper (ii) ions. *Analytical Methods* **2019**,*11* (5), 642-647.
27. Zhang, M.; Gong, L.; Sun, C.; Li, W.; Chang, Z.; Qi, D., A new fluorescent-colorimetric chemosensor based on a Schiff base for detecting Cr<sup>3+</sup>, Cu<sup>2+</sup>, Fe<sup>3+</sup> and Al<sup>3+</sup> ions. *Spectrochimica Acta Part A: Molecular and Biomolecular Spectroscopy* **2019**,*214*, 7-13.
28. Mahajan, P. G.; Bhopate, D. P.; Kolekar, G. B.; Patil, S. R., N-methyl isatin nanoparticles as a novel probe for selective detection of Cd<sup>2+</sup> ion in aqueous medium based on chelation enhanced fluorescence and application to environmental sample. *Sensors and Actuators B: Chemical* **2015**,*220*, 864-872.
29. Shellaiah, M.; Simon, T.; Sun, K. W.; Ko, F.-H., Simple bare gold nanoparticles for rapid colorimetric detection of Cr<sup>3+</sup> ions in aqueous medium with real sample applications. *Sensors and Actuators B: Chemical* **2016**,*226*, 44-51.
30. Shen, J.; Sun, C.; Wu, X., Silver nanoprisms-based Tb (III) fluorescence sensor for highly selective detection of dopamine. *Talanta* **2017**,*165*, 369-376.

31. Salimi, F.; Kiani, M.; Karami, C.; Taher, M. A., Colorimetric sensor of detection of Cr (III) and Fe (II) ions in aqueous solutions using gold nanoparticles modified with methylene blue. *Optik* **2018**,*158*, 813-825.
32. Wang, N.; Liu, Y.; Li, Y.; Liu, Q.; Xie, M., Fluorescent and colorimetric sensor for Cu<sup>2+</sup> ion based on formaldehyde modified hyperbranched polyethylenimine capped gold nanoparticles. *Sensors and Actuators B: Chemical* **2018**,*255*, 78-86.
33. Pinyorosphatum, C.; Rattanarat, P.; Chaiyo, S.; Siangproh, W.; Chailapakul, O., Colorimetric sensor for determination of phosphate ions using anti-aggregation of 2-mercaptoethanesulfonate-modified silver nanoplates and europium ions. *Sensors and Actuators B: Chemical* **2019**.
34. Wu, H.; Li, Y.; He, X.; Chen, L.; Zhang, Y., Colorimetric sensor based on 4-mercaptophenylboronic modified gold nanoparticles for rapid and selective detection of fluoride anion. *Spectrochimica Acta Part A: Molecular and Biomolecular Spectroscopy* **2019**,*214*, 393-398.
35. Ruecha, N.; Rodthongkum, N.; Cate, D. M.; Volckens, J.; Chailapakul, O.; Henry, C. S., Sensitive electrochemical sensor using a graphene–polyaniline nanocomposite for simultaneous detection of Zn (II), Cd (II), and Pb (II). *Analytica chimica acta* **2015**,*874*, 40-48.
36. Lin, Y.; Peng, Y.; Di, J., Electrochemical detection of Hg (II) ions based on nanoporous gold nanoparticles modified indium tin oxide electrode. *Sensors and Actuators B: Chemical* **2015**,*220*, 1086-1090.
37. Lee, S.; Oh, J.; Kim, D.; Piao, Y., A sensitive electrochemical sensor using an iron oxide/graphene composite for the simultaneous detection of heavy metal ions. *Talanta* **2016**,*160*, 528-536.
38. Romih, T.; Hočevár, S. B.; Kononenko, V.; Drobne, D., The application of bismuth film electrode for measuring Zn (II) under less acidic conditions in the presence of cell culture medium and ZnO nanoparticles. *Sensors and Actuators B: Chemical* **2017**,*238*, 1277-1282.
39. Shetti, N. P.; Nayak, D. S.; Malode, S. J.; Kulkarni, R. M., An electrochemical sensor for clozapine at ruthenium doped TiO<sub>2</sub> nanoparticles modified electrode. *Sensors and Actuators B: Chemical* **2017**,*247*, 858-867.

40. Liu, Y.; Lai, Y.; Yang, G.; Tang, C.; Deng, Y.; Li, S.; Wang, Z., Cd-aptamer electrochemical biosensor based on AuNPs/CS modified glass carbon electrode. *Journal of Biomedical Nanotechnology* **2017**,*13* (10), 1253-1259.
41. Simpson, A.; Pandey, R.; Chusuei, C. C.; Ghosh, K.; Patel, R.; Wanekaya, A. K., Fabrication characterization and potential applications of carbon nanoparticles in the detection of heavy metal ions in aqueous media. *Carbon* **2018**,*127*, 122-130.
42. Marie, M.; Manoharan, A.; Kuchuk, A.; Ang, S.; Manasreh, M., Vertically grown zinc oxide nanorods functionalized with ferric oxide for in vivo and non-enzymatic sglucose detection. *Nanotechnology* **2018**,*29* (11), 115501.
43. Cao, L.; Kiely, J.; Piano, M.; Luxton, R., Facile and inexpensive fabrication of zinc oxide based bio-surfaces for C-reactive protein detection. *Scientific reports* **2018**,*8* (1), 12687.
44. Zhu, X.; Zhang, K.; Wang, D.; Zhang, D.; Yuan, X.; Qu, J., Electrochemical sensor based on hydroxylated carbon nanotubes/platinum nanoparticles/rhodamine B composite for simultaneous determination of 2, 4, 6-trichlorophenol and 4-chlorophenol. *Journal of Electroanalytical Chemistry* **2018**,*810*, 199-206.
45. Chen, Y.; Zhang, D.; Wang, D.; Lu, L.; Wang, X.; Guo, G., A carbon-supported BiSn nanoparticles based novel sensor for sensitive electrochemical determination of Cd (II) ions. *Talanta* **2019**,*202*, 27-33.
46. Zainul, R.; Abd Azis, N.; Md Isa, I.; Hashim, N.; Ahmad, M. S.; Saidin, M. I.; Mukdasai, S., Zinc/Aluminium–Quinlorac Layered Nanocomposite Modified Multi-Walled Carbon Nanotube Paste Electrode for Electrochemical Determination of Bisphenol A. *Sensors* **2019**,*19* (4), 941.
47. Singh, A. C.; Asif, M.; Bacher, G.; Danielsson, B.; Willander, M.; Bhand, S., Nanoimmunosensor based on ZnO nanorods for ultrasensitive detection of 17 $\beta$ -Estradiol. *Biosensors and Bioelectronics* **2019**,*126*, 15-22.
48. Liao, Y.; Li, Q.; Wang, N.; Shao, S., Development of a new electrochemical sensor for determination of Hg (II) based on Bis (indolyl) methane/Mesoporous carbon nanofiber/Nafion/glassy carbon electrode. *Sensors and Actuators B: Chemical* **2015**,*215*, 592-597.

49. Zhang, C.; Li, L.; Ju, J.; Chen, W., Electrochemical sensor based on graphene-supported tin oxide nanoclusters for nonenzymatic detection of hydrogen peroxide. *Electrochimica Acta* **2016**,*210*, 181-189.
50. Zhou, W.; Li, C.; Sun, C.; Yang, X., Simultaneously determination of trace Cd<sup>2+</sup> and Pb<sup>2+</sup> based on l-cysteine/graphene modified glassy carbon electrode. *Food chemistry* **2016**,*192*, 351-357.
51. Sadak, O.; Sundramoorthy, A. K.; Gunasekaran, S., Highly selective colorimetric and electrochemical sensing of iron (III) using Nile red functionalized graphene film. *Biosensors and Bioelectronics* **2017**,*89*, 430-436.
52. Shi, R.; Liang, J.; Zhao, Z.; Liu, A.; Tian, Y., An electrochemical bisphenol A sensor based on one step electrochemical reduction of cuprous oxide wrapped graphene oxide nanoparticles modified electrode. *Talanta* **2017**,*169*, 37-43.
53. Dahaghin, Z.; Kilmartin, P. A.; Mousavi, H. Z., Simultaneous determination of lead (II) and cadmium (II) at a glassy carbon electrode modified with GO@ Fe<sub>3</sub>O<sub>4</sub>@ benzothiazole-2-carboxaldehyde using square wave anodic stripping voltammetry. *Journal of Molecular Liquids* **2018**,*249*, 1125-1132.
54. Gevaerd, A.; Blaskiewicz, S. F.; Zarbin, A. J.; Orth, E. S.; Bergamini, M. F.; Marcolino-Junior, L. H., Nonenzymatic electrochemical sensor based on imidazole-functionalized graphene oxide for progesterone detection. *Biosensors and Bioelectronics* **2018**,*112*, 108-113.
55. Dahaghin, Z.; Kilmartin, P. A.; Mousavi, H. Z., Determination of cadmium (II) using a glassy carbon electrode modified with a Cd-ion imprinted polymer. *Journal of Electroanalytical Chemistry* **2018**,*810*, 185-190.
56. Chen, Y.; Huang, W.; Chen, K.; Zhang, T.; Wang, Y.; Wang, J., A novel electrochemical sensor based on core-shell-structured metal-organic frameworks: The outstanding analytical performance towards chlorogenic acid. *Talanta* **2019**,*196*, 85-91.
57. Rawool, C. R.; Srivastava, A. K., A dual template imprinted polymer modified electrochemical sensor based on Cu metal organic framework/mesoporous carbon for highly sensitive and selective recognition of rifampicin and isoniazid. *Sensors and Actuators B: Chemical* **2019**.

58. Nourifard, F.; Payehghadr, M.; Kalhor, M.; Nejadali, A., An electrochemical sensor for determination of Ultratrace Cd, Cu and Hg in water samples by modified carbon paste electrode base on a new Schiff base ligand. *Electroanalysis* **2015**,*27* (10), 2479-2485.
59. Pazalja, M.; Kahrović, E.; Zahirović, A.; Turkušić, E., Electrochemical sensor for determination of L-cysteine based on carbon electrodes modified with Ru (III) Schiff base complex, carbon nanotubes and Nafion. *Int. J. Electrochem. Sci* **2016**,*11*, 10939-52.
60. Gorczyński, A.; Pakulski, D.; Szymańska, M.; Kubicki, M.; Bułat, K.; Łuczak, T.; Patroniak, V., Electrochemical deposition of the new manganese (II) Schiff-base complex on a gold template and its application for dopamine sensing in the presence of interfering biogenic compounds. *Talanta* **2016**,*149*, 347-355.
61. Ourari, A.; Ketfi, B.; Malha, S. I. R.; Amine, A., Electrocatalytic reduction of nitrite and bromate and their highly sensitive determination on carbon paste electrode modified with new copper Schiff base complex. *Journal of Electroanalytical Chemistry* **2017**,*797*, 31-36.
62. Yuan, G.; Tian, Y.; Liu, J.; Tu, H.; Liao, J.; Yang, J.; Yang, Y.; Wang, D.; Liu, N., Schiff base anchored on metal-organic framework for Co (II) removal from aqueous solution. *Chemical Engineering Journal* **2017**,*326*, 691-699.
63. Rahman, M. M.; Sheikh, T. A.; El-Shishtawy, R. M.; Arshad, M. N.; Al-Zahrani, F. A.; Asiri, A. M., Fabrication of Sb 3+ sensor based on 1, 1'-(-(naphthalene-2, 3-diylbis (azanylylidene)) bis (methanylylidene)) bis (naphthalen-2-ol)/nafion/glassy carbon electrode assembly by electrochemical approach. *RSC Advances* **2018**,*8* (35), 19754-19764.
64. Bharathi, K.; Kumar, S. P.; Prasad, P. S.; Narayanan, V., Voltammertic determination of paracetamol by N, N'-bis (salicylaldimine)-benzene-1, 2-diamine chromium (III) Schiff base complex modified GCE. *Materials Today: Proceedings* **2018**,*5* (2), 8961-8967.
65. Wang, L.; Gong, C.; Shen, Y.; Xu, M.; He, G.; Wang, L.; Song, Y., Conjugated schiff base polymer foam/macroporous carbon integrated electrode for electrochemical sensing. *Sensors and Actuators B: Chemical* **2018**,*265*, 227-233.

66. Mohan, C.; Sharma, K.; Kumari, S. In *Ion-Selective Electrode Based on Thiosemicarbazide Schiff Base As Ionophore for Pb (II) Ion Sensor*, Meeting Abstracts, The Electrochemical Society: 2019; pp 2029-2029.
67. Wang, L.; Xu, M.; Xie, Y.; Qian, C.; Ma, W.; Wang, L.; Song, Y., Ratiometric electrochemical glucose sensor based on electroactive Schiff base polymers. *Sensors and Actuators B: Chemical* **2019**,*285*, 264-270.
68. Aqlan, F. M.; Alam, M.; Asiri, A. M.; Zayed, M. E.; Al-Eryani, D. A.; Al-Zahrani, F. A.; El-Shishtawy, R. M.; Uddin, J.; Rahman, M. M., Fabrication of selective and sensitive Pb<sup>2+</sup> detection by 2, 2'-((1, 2-phenylenebis (azaneylylidene)) bis (methaneylylidene)) diphenol by electrochemical approach for environmental remediation. *Journal of Molecular Liquids* **2019**,*281*, 401-406.
69. Izadkhah, V.; Farmany, A.; Mortazavi, S., Voltammetric determination of copper in water samples using a Schiff base/carbon nanotube-modified carbon paste electrode. *Journal of Industrial and Engineering Chemistry* **2015**,*21*, 994-996.
70. Parsaei, M.; Asadi, Z.; Khodadoust, S., A sensitive electrochemical sensor for rapid and selective determination of nitrite ion in water samples using modified carbon paste electrode with a newly synthesized cobalt (II)-Schiff base complex and magnetite nanospheres. *Sensors and Actuators B: Chemical* **2015**,*220*, 1131-1138.
71. Jahani, S.; Beitollahi, H., Selective detection of dopamine in the presence of uric acid using nio nanoparticles decorated on graphene nanosheets modified screen-printed electrodes. *Electroanalysis* **2016**,*28* (9), 2022-2028.
72. Chaiyo, S.; Mehmeti, E.; Žagar, K.; Siangproh, W.; Chailapakul, O.; Kalcher, K., Electrochemical sensors for the simultaneous determination of zinc, cadmium and lead using a Nafion/ionic liquid/graphene composite modified screen-printed carbon electrode. *Analytica chimica acta* **2016**,*918*, 26-34.
73. Beitollahi, H.; Garkani Nejad, F., Graphene oxide/ZnO nano composite for sensitive and selective electrochemical sensing of levodopa and tyrosine using modified graphite screen printed electrode. *Electroanalysis* **2016**,*28* (9), 2237-2244.

74. Rana, S.; Mittal, S. K.; Singh, N.; Singh, J.; Banks, C. E., Schiff base modified screen printed electrode for selective determination of aluminium (III) at trace level. *Sensors and Actuators B: Chemical* **2017**,*239*, 17-27.
75. Mehta, J.; Bhardwaj, N.; Bhardwaj, S. K.; Tuteja, S. K.; Vinayak, P.; Paul, A.; Kim, K.-H.; Deep, A., Graphene quantum dot modified screen printed immunosensor for the determination of parathion. *Analytical biochemistry* **2017**,*523*, 1-9.
76. Reddy, Y. V. M.; Sravani, B.; Agarwal, S.; Gupta, V. K.; Madhavi, G., Electrochemical sensor for detection of uric acid in the presence of ascorbic acid and dopamine using the poly (DPA)/SiO<sub>2</sub>@ Fe<sub>3</sub>O<sub>4</sub> modified carbon paste electrode. *Journal of Electroanalytical Chemistry* **2018**,*820*, 168-175.
77. Jian, J.-M.; Fu, L.; Ji, J.; Lin, L.; Guo, X.; Ren, T.-L., Electrochemically reduced graphene oxide/gold nanoparticles composite modified screen-printed carbon electrode for effective electrocatalytic analysis of nitrite in foods. *Sensors and Actuators B: Chemical* **2018**,*262*, 125-136.
78. Jeromiyas, N.; Elaiyappillai, E.; Kumar, A. S.; Huang, S.-T.; Mani, V., Bismuth nanoparticles decorated graphenated carbon nanotubes modified screen-printed electrode for mercury detection. *Journal of the Taiwan Institute of Chemical Engineers* **2019**,*95*, 466-474.
79. Baccarin, M.; Rowley-Neale, S. J.; Cavalheiro, É. T.; Smith, G. C.; Banks, C. E., Nanodiamond based surface modified screen-printed electrodes for the simultaneous voltammetric determination of dopamine and uric acid. *Microchimica Acta* **2019**,*186* (3), 200.
80. Rosal, M.; Cetó, X.; Serrano, N.; Ariño, C.; Esteban, M.; Díaz-Cruz, J. M., Dimethylglyoxime modified screen-printed electrodes for nickel determination. *Journal of Electroanalytical Chemistry* **2019**.
81. Parsa, A.; Akbarzadeh-Torbati, N.; Beitollahi, H., Rapid and Sensitive Electrochemical Monitoring of Tyrosine Using NiO Nanoparticles Modified Graphite Screen Printed Electrode. *INTERNATIONAL JOURNAL OF ELECTROCHEMICAL SCIENCE* **2019**,*14* (1), 1556-1565.

82. Yao, Y.; Wu, H.; Ping, J., Simultaneous determination of Cd (II) and Pb (II) ions in honey and milk samples using a single-walled carbon nanohorns modified screen-printed electrochemical sensor. *Food chemistry* **2019**,*274*, 8-15.
83. Burgoa, M. C.; Domínguez, O. R.; Arcos, M. M., Determination of lamotrigine by adsorptive stripping voltammetry using silver nanoparticle-modified carbon screen-printed electrodes. *Talanta* **2007**,*74* (1), 59-64.
84. Singh, S.; Meena, V.; Mizaikoff, B.; Singh, S.; Suri, C., Electrochemical sensing of nitro-aromatic explosive compounds using silver nanoparticles modified electrochips. *Analytical Methods* **2016**,*8* (39), 7158-7169.
85. Yagmur, S.; Yilmaz, S.; Saglikoglu, G.; Sadikoglu, M.; Yildiz, M.; Polat, K., Synthesis, spectroscopic studies and electrochemical properties of Schiff bases derived from 2-hydroxy aromatic aldehydes and phenazopyridine hydrochloride. *Journal of the Serbian Chemical Society* **2013**,*78* (6), 795.
86. Rana, S.; Mittal, S. K.; Kaur, N.; Banks, C. E., Disposable screen printed electrode modified with imine receptor having a wedge bridge for selective detection of Fe (II) in aqueous medium. *Sensors and Actuators B: Chemical* **2017**,*249*, 467-477.
87. Mistry, K. K.; Sagarika Deepthy, T.; Chaudhuri, C. R.; Saha, H., Electrochemical characterization of some commercial screen-printed electrodes in different redox substrates. *Current science* **2015**, 1427-1436.
88. Kumar, S.; Mittal, S. K.; Kaur, N.; Kaur, R., Improved performance of Schiff based ionophore modified with MWCNT for Fe (II) sensing by potentiometry and voltammetry supported with DFT studies. *RSC Advances* **2017**,*7* (27), 16474-16483.



## Msc thesis

### ORIGINALITY REPORT

14%

SIMILARITY INDEX

8%

INTERNET SOURCES

11%

PUBLICATIONS

9%

STUDENT PAPERS

### PRIMARY SOURCES

- 1** Yao, Xianzhi, Zheng Guo, Qing-Hong Yuan, Zhong-Gang Liu, Jin-Huai Liu, and Xing-Jiu Huang. "Exploiting Differential Electrochemical Stripping Behaviors of Octahedral Fe<sub>3</sub>O<sub>4</sub> Nanocrystals toward Heavy Metal Ions by Crystal Cutting", ACS Applied Materials & Interfaces  
Publication 1%
- 2** Cao, Wei, Xiang-Jun Zheng, Ji-Ping Sun, Wing-Tak Wong, De-Cai Fang, Jia-Xin Zhang, and Lin-Pei Jin. "A Highly Selective Chemosensor for Al(III) and Zn(II) and Its Coordination with Metal Ions", Inorganic Chemistry, 2014.  
Publication <1%
- 3** www.mdpi.com  
Internet Source <1%
- 4** Susheel K. Mittal, Rashmi Sharma, Manisha Sharma, Narinder Singh, Jasminder Singh, Navneet Kaur, Manmohan Chhibber.  
"Voltammetry of nanoparticle-coupled imine <1%

*many smart  
such pages  
11 than 1%*

*Susheel mittal*